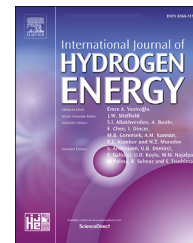


Available online at [www.sciencedirect.com](http://www.sciencedirect.com)

ScienceDirect

journal homepage: [www.elsevier.com/locate/he](http://www.elsevier.com/locate/he)

# Assessment of power-to-power renewable energy storage based on the smart integration of hydrogen and micro gas turbine technologies



Antonio Escamilla<sup>\*</sup>, David Sánchez, Lourdes García-Rodríguez

University of Seville (Department of Energy Engineering), Camino de los Descubrimientos s/n, Spain

## HIGHLIGHTS

- Round-trip efficiency of P2P energy storage system with micro gas turbines between 22% and 29%.
- Literature review of hydrogen electrolysis systems available in the market.
- Thermodynamic analysis of H<sub>2</sub> compression with a specific energy consumption of around 10% of H<sub>2</sub> energy content.
- Hydrogen storage in high-pressure vessels, liquefied and in metal hydrides.
- Hydrogen transportation by Fuel Cell Electric Truck for an average distance of 200 km per trip.

## ARTICLE INFO

### Article history:

Received 4 January 2022

Received in revised form

22 March 2022

Accepted 23 March 2022

Available online 15 April 2022

### Keywords:

Power-to-Power

Micro-gas turbines

Renewable hydrogen

Energy storage systems

## ABSTRACT

Power-to-Power is a process whereby the surplus of renewable power is stored as chemical energy in the form of hydrogen. Hydrogen can be used in situ or transported to the consumption node. When power is needed again, hydrogen can be consumed for power generation. Each of these processes incurs energy losses, leading to a certain **round-trip efficiency** (Energy Out/Energy In). Round-trip efficiency is calculated considering the following processes; water electrolysis for hydrogen production, compressed, liquefied or metal-hydride for hydrogen storage, fuel-cell-electric-truck for hydrogen distribution and micro-gas turbine for hydrogen power generation. The maximum achievable round-trip efficiency is of 29% when considering solid oxide electrolysis along with metal hydride storage. This number goes sharply down when using either alkaline or proton exchange membrane electrolyzers, 22.2% and 21.8% respectively. Round-trip efficiency is further reduced if considering other storage media, such as compressed- or liquefied-H<sub>2</sub>. However, the aim of the paper is to highlight there is still a large margin to increase Power-to-Power round-trip efficiency, mainly from the hydrogen production and power generation blocks, which could lead to round-trip efficiencies of around 40%–42% in the next decade for Power-to-Power energy storage systems with micro-gas turbines.

© 2022 The Authors. Published by Elsevier Ltd on behalf of Hydrogen Energy Publications LLC. This is an open access article under the CC BY-NC-ND license (<http://creativecommons.org/licenses/by-nc-nd/4.0/>).

<sup>\*</sup> Corresponding author.

E-mail address: [a.escamilla@us.es](mailto:a.escamilla@us.es) (A. Escamilla).

<https://doi.org/10.1016/j.ijhydene.2022.03.238>

0360-3199/© 2022 The Authors. Published by Elsevier Ltd on behalf of Hydrogen Energy Publications LLC. This is an open access article under the CC BY-NC-ND license (<http://creativecommons.org/licenses/by-nc-nd/4.0/>).

### Glossary

|       |   |
|-------|---|
| AEC   | Alkaline Electrolyser                   |
| BoP   | Balance of Plant                        |
| CA    | Compressed Air                          |
| CAES  | Compressed Air Energy Storage           |
| CapEx | Capital Expenditure                     |
| CCS   | Carbon Capture and Sequestration        |
| CHP   | Combined Heat and Power                 |
| EC    | Electrolyser                            |
| ESS   | Energy Storage Systems                  |
| FC    | Fuel Cell                               |
| FCET  | Fuel Cell Electric Truck                |
| GHG   | Greenhouse Gases                        |
| GT    | Gas Turbine.                            |
| LAES  | Liquid Air Energy Storage               |
| LCOH  | Levelized Cost of Hydrogen              |
| mGT   | micro-Gas Turbine.                      |
| MH    | Metal Hydride.                          |
| OEM   | Original Equipment Manufacturer         |
| OpEx  | Operational Expenditure                 |
| P2P   | Power-to-Power                          |
| P2X   | Power-to-X.                             |
| PEMEC | Proton Exchange Membrane Electrolyser   |
| PHS   | Pumped Hydroelectric Storage            |
| PtG   | Power-to-Gas                            |
| RES   | Renewable Energy Sources                |
| SEC   | Specific Energy Consumption             |
| SMES  | Superconducting Magnetic Energy Storage |
| SOEC  | Solid Oxide Electrolyser                |
| SOFC  | Solid Oxide Fuel Cell                   |
| VRE   | Variable Renewable Energy               |

## Introduction

The interest in Power-to-Power energy storage systems has been increasing steadily in recent times, in parallel with the also increasingly larger shares of variable renewable energy (VRE) in the power generation mix worldwide [1]. Owing to the characteristics of VRE, adapting the energy market to a high penetration of VRE will be of utmost importance in the coming years [2]. Variable renewable energies like wind or solar are characterised for being an intermittent source of energy whose availability for power generation depends mainly on local weather conditions, which can be predicted accurately 24–36 h in advance only [3]. This, along with the very limited options for large-scale energy storage available today and the increasingly larger share of VREs into the energy mix, implies that the grid must still rely on conventional power generation technologies to generate electricity when VRE is not available. These conventional power generation technologies are very reliable but they also feature high emissions of greenhouse gases (GHG) and, in some cases, other hazardous emissions like nuclear waste. Large-scale energy storage is thus one of the most pressing technical challenges to achieve carbon-neutrality by 2050. Additionally, and parallel to this, smart energy systems for managing production, distribution and

consumption of electricity, heat, and gas are of prime importance to enable a 100% renewable energy scenario [4,5].

Energy Storage Systems (ESS) are usually classified according to the form in which energy is stored: *electrical, electrochemical, chemical, mechanical* and *thermal*. An explanation of each of these ESSs is found at [6,7] along with a summary of their main characteristics. Amongst all these, there are only two ESSs which have so far met the requirements for a successful deployment of large-scale energy storage to the market, and both are of the *mechanical* type: pumped-hydro and compressed-air. Pumped Hydroelectric Storage (PHS) is the oldest and most mature technology. It represents the largest form of storage today, accounting for 96% of the total energy storage capacity amongst all technologies [8]. Nevertheless, PHS is strongly dependent on local geographic features as it requires the presence of both water streams and natural/artificial basins with large differences in altitude. This poses obvious restrictions on the large-scale deployment of PHS systems. Compressed Air Energy Storage (CAES) has similar limitations since its technical and economic feasibility is limited to locations where large caverns are available [9].

In addition to these two ESS technologies, there are other options for energy storage but they are presently applicable at the small-scale only: electrochemical batteries, flow batteries, Superconducting Magnetic Energy Storage systems (SMES), flywheels, capacitors and supercapacitors. With such limitations, these technologies seem to be more suitable for grid balance when needed than for large-scale energy storage. Nevertheless, with these caveats and despite a lower maturity and somewhat difficult scalability, chemical energy storage has gained interest in recent years. This is partly due to the noteworthy development of larger-scale water electrolysis technologies and to the penetration of Renewable Energy Sources (RES) in the energy mix, which seem to make it technically possible in the near future to produce large amounts of hydrogen using RES only as secondary form of energy [10].<sup>1</sup> This hydrogen is termed green-hydrogen and the associated energy (hydrogen) storage technology from RES is known as Power-to-Hydrogen (PtG-Hydrogen). The main advantage of this ESS is that hydrogen is an energy carrier which can be stored, transported, and converted into other forms of energy such as mechanical, power, heat, etc.

Unlike PHS or CAES, hydrogen can be produced *in-situ* wherever there are power and water supplies. It can also be stored in different forms (gas distribution network, high-pressure tanks, metal hydrides ...) and not only can it be delivered in the form of electric power but it can also be converted into mechanical power (mobility), thermal energy (heating networks, process heat ...) or even as feedstock for the industry (oil refineries). Thus, even though this work is focused on applications where hydrogen is converted back into electric power through combustion in micro gas turbines, the interest in hydrogen technologies does not limit to electrification but these are also seen as a means to help decarbonise those sectors where electrification is not feasible. The production of hydrogen from water electrolysis using RES and

<sup>1</sup> Water electrolysis is well established today but mass-production of electrolyzers is still a bottle neck for the implementation of this energy storage technology at the large scale.

**Table 1 – Power-to-X projects under development around the world.**

| Project Name       | Location |                    | (X) Product                      | Reinjection | Start | Power |
|--------------------|----------|--------------------|----------------------------------|-------------|-------|-------|
|                    | Country  | City               |                                  | Yes/No      | Year  | MWe   |
| FLEXnCONFU [21]    | PT       | Lisbon             | H <sub>2</sub> , NH <sub>3</sub> | No          | 2020  | 1     |
| HYFLEXPOWER [22]   | FR       | Saillat-sur-Vienne | H <sub>2</sub>                   | No          | 2020  | 12    |
| ROBINSON [19]      | NW       | Eigerøy            | H <sub>2</sub> , Biogas          | Yes         | 2020  | 0.4   |
| ACES [18]          | US       | Utah               | H <sub>2</sub> , CA              | Yes         | 2019  | 1000  |
| GREEN HYSLAND [20] | SP       | Majorca            | H <sub>2</sub>                   | Yes         | 2021  | –     |

its later use for power generation is termed Power-to-Power (P2P).

Numerous research projects on the topic (power-to-hydrogen) have been developed in recent years, both theoretically and experimentally. In this latter group, around 143 PtG projects producing either hydrogen or methane have been operated in the last decades, some of them starting as far back as 1988 [11,12]. Most of these facilities were pilot or demonstration plants with power ratings under 1MWe, aimed at enabling a more profound understanding of the practical challenges and technical gaps that still need further research. As of 2019, there were 56 active PtG projects based on hydrogen, with an installed electric capacity of 24.1MWe [11]. Germany hosts the largest number of these plants, with 64 PtG projects, but the stimulus given by governments around the world will expectedly see other countries catching up in the next years [13–16].

The estimated worldwide production of hydrogen by the end of 2018 was 74 Mt, 97% of which was produced through steam reforming of natural gas (methane) and, therefore, with large emissions of carbon dioxide. Most of this hydrogen was actually not traded or distributed but, on the contrary, it was produced locally for refineries and for the production of ammonia [2,17]. From these values, hydrogen production worldwide is expected to reach 240 Mt by 2050 [2], when it will play a key role in the mobility, power and heat sectors even if this production would cover 7.5% of the global energy demand worldwide only. In addition, it goes without saying that significant efforts have to be made to achieve this target, both technical and economic, amongst which the installation of 50 GWe to 60 GWe electrolyser capacity annually.

As a consequence of the large effort to scale-up technologies that enable the utilisation of hydrogen as an energy carrier, applications where hydrogen can help to achieve carbon-neutrality are flourishing. More than twenty applications where hydrogen can become a cost-competitive low-carbon solution before 2030 have been identified in a recent report by the Hydrogen Council [10], needing a large investment effort if they are to be developed and taken to the market. Approximately EUR 60 billion investment is required by 2030 to achieve cost-effectiveness of hydrogen technologies, which can be facilitated through the following five drivers: reduced market uncertainty, larger *improvement-for-investments* for technology boost, hybrid solutions, increasing utilisation rates in distribution networks and investments in blue/green

hydrogen.<sup>2</sup> Along with these, other actions aimed at setting common policies to nurture a favourable ecosystem for the commercial deployment of hydrogen are needed. In particular, governments are expected to work on the following areas to unfold aligned policies: national strategies, coordination, regulation, standardisation, infrastructures and incentives.

From a supply-chain standpoint, the research of P2P solutions can be categorised into hydrogen production, storage and consumption. For production: direct coupling between RES and electrolyser (EC), high temperature electrolysis, and footprint and materials of ECs are currently attracting significant efforts. For storage: higher storage capability at higher pressure (> 60 kg<sub>H<sub>2</sub></sub> at >700 bar), metal hydrides, NG-H<sub>2</sub> blends in gas grids. For power generation: hydrogen combustion, high temperature fuel cells, hybrid systems (not only integration concepts but also control systems, power electronics, and other auxiliary systems).

Table 1 contains a summary of the main Power-to-X (P2X) projects that are currently under development, X being any form of energy. Although all of them consider the production of hydrogen through water electrolysis, they differ from one another in the hydrogen storage solution, power rating and target sector (mobility or industry). Indeed, different scales can be observed, from small systems (0.4MWe) to very large hydrogen infrastructures like the Advanced Clean Energy Storage (ACES) [18] project in central Utah, which is considered the “World's largest” energy storage project planned (1GWe rated electrolyser capacity). ACES will make use of three storage technologies: renewable hydrogen that is then converted into electric power with a hybrid system comprised of solid oxide fuel cells and gas turbines, CAES and large-scale flow batteries. In addition to this, due to the importance of decentralised power generation, there are other projects which cover smaller energy storage capacities, for instance ROBINSON [19] and GREEN HYSLAND [20]. Their main target is to optimise the utilisation of local RES by deploying an integrated, smart and cost-effective energy system coupling thermal and electrical networks.

There number of studies in literature dealing with different subjects within the concept of P2X is very large. Heyman et al. present a flexible framework to compare the performance of power-to-gas sites, providing useful indicators about energy conversion technologies, plant size, cost structure, and configuration [23]. Crespi et al. compare the use of hydrogen-based P2P systems, battery systems and hybrid hydrogen-battery systems to supply a constant 1 MW<sub>el</sub> load with electricity locally generated by a photovoltaic plant [24]. In this work, systems are sized in order to minimize the annual average cost of electricity. Loisel et al. also deal with an

<sup>2</sup> The term *blue* hydrogen refers to hydrogen that is produced through conventional steam reforming and downstream carbon capture, utilisation and storage, hence with no net carbon emissions.

economic evaluation to predict the LCOH for different scenarios in France [25]. The authors conclude that, for the different scenarios considered, LCOH would be in the range from 4 to 13 €/kg H<sub>2</sub>. Bexten et al. focus on the economic viability of the on-site hydrogen supply for an industrial gas turbine, analysing the impact of parameters such as number of wind turbines, available EC capacity and hydrogen storage capacity [26]. It is concluded that with the current economic framework, the solution is not economically viable. Focusing more on thermodynamic features, Mukelabai et al. deal with power-to-ammonia and ammonia-to-power systems using a reversible solid oxide system, reporting round-trip efficiencies between 41 and 53% for the cases considered [27]. Wang et al. make use of a thermodynamic analysis to compare different fuels in a power-to-X-to-power system using a reversible solid oxide cell [28]. The work reports the following round-trip efficiencies for the different systems considered: 47.5% (methane), 43.4% (syngas), 42.6% (hydrogen), 40.7% (methanol), and 38.6% (ammonia). Ishaq et al. investigate the performance of an integrated wind energy system producing hydrogen and power through a PEMEC and FC [29], reporting energy and exergy efficiencies of the system against wind speed.

More complex cycle layouts to increase energy and exergy efficiencies are proposed by other authors. Motahar et al. look into the 2nd Law performance of a hybrid system comprised of an SOFC and steam injected gas turbine, determining that both the combustion chamber and fuel cell stack are the components with highest exergy destruction [30]. Alirahmi et al. consider an integrated FC/geothermal-based energy system generating cool power and electricity at the same time [31]. The system is driven by geothermal energy and the electricity is mostly produced by a dual organic cycle. An EC is used to produce hydrogen which is later used by a FC to support the grid during peak consumption periods. This yields minimum cost rate and maximum exergy efficiency. Additionally, Tukenmez et al. propose a layout consisting of the following subsystems: gas turbine cycle, Rankine cycle, two organic Rankine cycles, ejector-based cooling, hydrogen production and liquefaction, ammonia production and storage, drying, and hot water generation [32]. It reports overall energy and exergy efficiencies of 62% and 58%, respectively.

The current work is aimed at the assessment of power-to-hydrogen-to-power (P2P) energy storage systems as an

efficient means to reliably increase the share of renewable energies in the grid. In contrast with most of the works on P2P systems available in literature, focusing more on global techno-economic considerations and disregarding the fundamentals of the technology, the main goal of this analysis is to look into the thermodynamic principles of each process along the value-chain of hydrogen with the aim to characterise the energy balance of this energy storage option. This yields a much more accurate calculation of the round-trip efficiency, figure of merit usually adopted to compare the efficiency of energy storage systems. Additionally, the study is restrained to using micro-gas turbines as a means to produce power from hydrogen. Hence, the P2P system considered here is limited to a maximum power output of around 500 kW<sub>e</sub>.

The paper is organised as follows. Section **Introduction** provides a comprehensive literature review of P2P systems and technologies with the aim to show that this work comes to fill a gap in the existing body of knowledge. Section **Power-to-hydrogen-to-power** presents the concept of P2P based on micro gas turbines, and provides the thermodynamic grounds for each of the systems involved. Section **Analysis** provides an energy balance of all the systems involved in the P2P energy storage section, identifying those systems where there is a larger room for optimisation to attain the highest round-trip efficiency possible. Finally, in Section **Discussion of results**, the results obtained and the different scenarios of improvement for each of the systems involved are discussed.

## Power-to-hydrogen-to-power

Power-to-Power (P2P) is a process whereby surplus renewable power is curtailed through conversion into chemical energy (in the case of interest for this paper, hydrogen) for storage. This stored energy can later be used *in-situ* or transported to a consumption node. This can be achieved by using hydrogen as a fuel for power generation in either thermo-mechanical (i.e., heat engines) or electrochemical (i.e., fuel cells) devices or, less often, through direct conversion into heat. Four separate processes can hence be identified to assess energy losses of the entire setup: production, storage, transportation/distribution and power generation (Fig. 1). Each of these processes incurs energy losses, leading to a certain global or round-trip

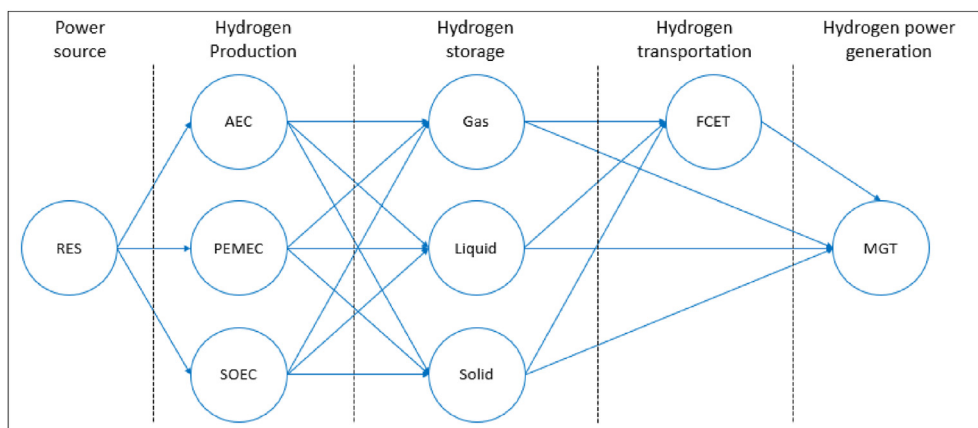
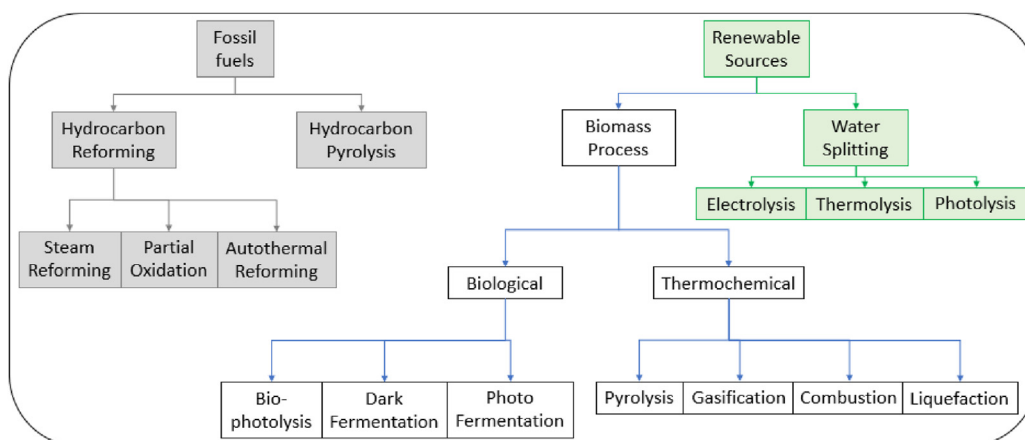


Fig. 1 – Power-to-Power options considered.



**Fig. 2 – Hydrogen production methods. Colour code: green and grey refer to the origin of the primary energy used for hydrogen production, as noted in the figure. (For interpretation of the references to colour in this figure legend, the reader is referred to the Web version of this article.)**

efficiency representing the fraction of energy originally taken from the grid (or source of electric energy) that is delivered back to it. The following sections deal with the different aspects involved in the calculation of round-trip efficiency of the power-to-power solutions considered in this work.

### Hydrogen production

Hydrogen is not found in free molecular form on Earth but, rather, bounded to other elements in the form of stable compounds, for instance hydrocarbons. Hence, chemical processes are needed to obtain molecular hydrogen,  $H_2$ , and they all require a non-negligible supply of primary energy. Fig. 2 summarises the alternatives that have been investigated so far.

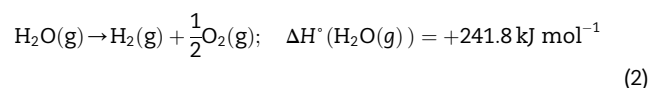
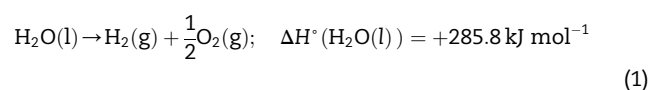
The following terminology or colour code is commonly used to refer to different hydrogen production processes [17]:

- Brown hydrogen: the primary energy source is coal and the specific emissions of the process are estimated at  $19 t_{CO_2}/t_{H_2}$ .
- Grey hydrogen: the primary energy source is natural gas and the specific emissions of the process are estimated at  $11 t_{CO_2}/t_{H_2}$ .
- Blue hydrogen: same as grey hydrogen but incorporating Carbon Capture and Sequestration (CCS) techniques. Specific emissions decrease to  $0.2 t_{CO_2}/t_{H_2}$ .
- Green hydrogen: renewable energy sources RES are used in this case so the associated carbon footprint is potentially null.

The vast majority of hydrogen produced in the world today (95%–97%) is grey hydrogen. This is owed to the reliability and scalability of steam reforming to produce hydrogen from natural gas, and to the much lower costs of this technology as opposed to other options to produce green hydrogen. In particular, grey hydrogen is 5–8 times cheaper than green hydrogen according to several techno-economic assessments of the technology [2,10,17]. Nevertheless, despite not being cost-effective today, only green hydrogen will be considered

in this document given the target to achieve net-zero emissions by 2050 set forth in the Paris Agreement [33]. Readers interested in other technologies are referred to the bibliography [34–36].

Water electrolysis is the dominant technology for the production of green hydrogen owing to its fairly high conversion efficiency and direct use of electricity, as opposed to other technologies which rely mostly on heat. This is a thermochemical process whereby electricity is consumed to split the water molecule into hydrogen and oxygen. The reaction is carried out in an electrolyser, which is an electrochemical device comprised of two electrodes where the half-reactions of oxidation and reduction take place, and of an ion-conductive electrolyte in between. The overall reaction and the total energy required to split 1 mol of  $H_2O$  at standard pressure and temperature (298.15 K and 1 bar) reversibly are:



The application of Gibbs-Helmholtz equation reveals the constituents of the total energy supply ( $\Delta H^\circ(H_2O(l))$ ):

$$\Delta H^\circ(H_2O(l)) = \Delta G^\circ(H_2O(l)) + T \cdot \Delta S^\circ(H_2O(l)) \quad (3)$$

where:

- $\Delta H^\circ(H_2O(l)) = 285.8 \text{ kJ mol}^{-1}$  is the total energy supply to the electrolyser.
- $\Delta G^\circ(H_2O(l)) = 237.2 \text{ kJ mol}^{-1}$  is the reversible electric work that must be supplied to the electrolyser to split the water molecule.
- $T \cdot \Delta S^\circ(H_2O(l)) = 48.6 \text{ kJ mol}^{-1}$  is the reversible heat (thermal energy) that must be supplied to the electrolyser to split the water molecule if the reaction is to be kept at constant temperature.

The minimum amount of electricity needed by the electrolyser to split the water molecule is  $\Delta G$  ( $\text{H}_2\text{O}(\text{l})$ ). Nevertheless, if no additional energy (either electrical or thermal) is supplied, the products will be colder than the reactants and the electrolyser will eventually cool down and come to a halt. Hence, in order to ensure operation at constant temperature,  $T \cdot \Delta S(\text{H}_2\text{O}(\text{l}))$  must also be supplied to the system.

Operation of the electrolyser at constant temperature is called thermoneutral operation and, when carried out reversibly, determines the minimum amount of energy that must be supplied to the electrolyser for sustained operation:  $285.8 \text{ kJ mol}^{-1}$  if water is supplied as a liquid or  $241.8 \text{ kJ mol}^{-1}$  if the feed is vapour. Based on this energy balance, the energy efficiency of an electrolyser is defined as follows:

$$\eta_{\text{LHV}} = \frac{\dot{m}_{\text{H}_2} \cdot \text{LHV}}{\dot{W}_{\text{el}} + \dot{Q}} \quad (4)$$

$$\eta_{\text{HHV}} = \frac{\dot{m}_{\text{H}_2} \cdot \text{HHV}}{\dot{W}_{\text{el}} + \dot{Q}} \quad (5)$$

Energy efficiency can be defined in terms of the produced chemical energy referred to either the high or low heating values of hydrogen,  $\eta_{\text{HHV}}$  and  $\eta_{\text{LHV}}$  respectively, though the former case is used more often ( $\eta_{\text{HHV}}$ ). As the electrochemical losses of the electrolyser cell increase, the consumption of electrical work increases with respect to the aforesaid value ( $237.2 \text{ kJ mol}^{-1}$  at standard pressure and temperature) and efficiency decreases accordingly.

The electrical work consumed by a cell can also be expressed in terms of voltage ( $V_{\text{cell}}$ ) and electric current ( $i_{\text{cell}}$ ):

$$W_{\text{el}} = V_{\text{cell}} \cdot i_{\text{cell}} = V_{\text{cell}} \cdot j \cdot A_{\text{cell}} \quad (6)$$

In Eq. (6),  $j$  and  $A_{\text{cell}}$  are the current density and active area of the electrolyser cell. The application of Nernst equation links Eqs. (6) and (3) to obtain the relationship between cell voltage and energy exchange:

$$V_{\text{rev}} = \frac{\Delta G}{n \cdot F} \quad (7)$$

$$V_{\text{tn}} = \frac{\Delta H}{n \cdot F} \quad (8)$$

The minimum voltage difference between electrodes splitting the water molecule in a reversible cell is  $V_{\text{rev}}$  (Eq. (7)<sup>3</sup>). In these conditions, an amount of thermal energy equal to  $T \cdot \Delta S$  must be supplied to the cell in order to keep temperature constant. Otherwise, a higher voltage must be applied and the excess electricity with respect to the former value is converted into heat. The latter voltage is termed thermal-neutral voltage  $V_{\text{tn}}$  (Eq. (8)). When the process is not reversible, a higher cell voltage is needed and a voltage efficiency can be defined as follows:

$$\eta_{\text{rev}} = \frac{V_{\text{rev}}}{V_{\text{cell}}} \quad (9)$$

$$\eta_{\text{tn}} = \frac{V_{\text{tn}}}{V_{\text{cell}}} \quad (10)$$

Again, this voltage efficiency can be defined with reference to the reversible cell voltage (Eq. (9)) or the thermoneutral voltage (Eq. (10)).

There are several electrolyser types, classified according to the nature (composition) of the electrolyte, given that this determines the half-reactions taking place at each electrode and the associated operating temperature and pressure. Nowadays, research is mostly focused on three electrolyser technologies: alkaline (AEC), proton-exchange membrane (PEMEC) and solid oxide (SOEC). Table 2 shows the main characteristics of each electrolyser type.

The most mature technology is AEC and it yields the lowest capital cost (CapEx). AEC is more appropriate for stationary applications where the operating conditions remain steady and load changes are slow, owing to their large footprint and difficulty to cope with steep thermal transients. PEMECs are characterised by a smaller footprint and much better response to rapid load changes. However, the Capital Cost (CapEx) of PEMECs is 2–3 times higher than for AEC, even if this figure is expected to decrease to some 600–1300 €/kW in the following decade [17,37,38]. The least mature technology amongst the three is SOEC. The working conditions of this type of electrolyser are totally different to the previous two since water must be provided in the form of steam at around 800°C and this requires a significant consumption of energy externally to the electrolyser stack. Interestingly though, the energy required to sustain the water electrolysis reaction is fairly constant in the range from 0°C to 1000°C [42], meaning that the higher consumption of heat (to produce steam in lieu of hot water) is compensated for by a much lower consumption of electricity. The net result is that the efficiency of SOEC is above 80% referred to the Low Heating Value (LHV) of hydrogen and close to 100% when considering the High Heating Value (HHV), given that the total energy consumption remains approximately constant in the aforesaid temperature range. This stems as an advantage over the other electrolyser technologies but working at such high temperature requires an external heat source (not electricity only as AEC and PEMEC) also brings problems associated with heat management and, of course, more costly materials.

Regarding the response time and start-up/shutdown capability (i.e., flexibility) of these types of ECs, both AEC and PEMEC are rather quick and flexible in a wide output range (5–10 to 100% load). Eichman et al. provide information about the response time for different changes in power setting and

**Table 2 – Characteristics of different types of electrolyser [37–41].**

| Parameter           | Unit                            | AEC       | PEMEC        | SOEC     |
|---------------------|---------------------------------|-----------|--------------|----------|
| T                   | °C                              | 60–80     | 50–80        | 650–1000 |
| P                   | Bar                             | 1–30      | 30–80        | 1        |
| j                   | A/cm <sup>2</sup>               | 0.5–1.0   | 2.0–3.0      | 2.0      |
| V                   | V                               | 1.75–2.40 | 1.6–2.0      | 1.2–1.3  |
| SEC                 | kWh/kg <sub>H<sub>2</sub></sub> | 51        | 70–55        | 41–40    |
| $\eta_{\text{HHV}}$ | %                               | 77        | 57–72        | 98       |
| CapEx               | €/kW                            | 750       | 1200–2000    | > 4500   |
| Regulation speed    | [order of] seconds              | seconds   | Milliseconds | hours    |
| Minimum load        | % full load                     | 10–20     | 0–5          | 30       |
| Lifetime            | Hours                           | 100 000   | 90 000       | 25 000   |

<sup>3</sup>  $F \equiv$  Faraday constant =  $96\,500 \text{ C mol}^{-1}$

also the time that is needed to start-up and shutdown the system [43]. These studies report that the settling time after a load change is in the order of seconds whereas start-up and shutdown is in the order of minutes. Hence, AEC and PEMEC are eligible for a very wide range of applications, including direct coupling to RES, as well as in the different electricity markets [37]. On the contrary, even if SOEC adapts rather quickly to changes in load setting, both the response and start-up/shutdown times range from minutes to hours to prevent the drastic reduction in the lifetime of components caused by fast temperature gradients [40,41].

Table 3 presents technical specifications taken from Original Equipment Manufacturers (OEMs) of different types of electrolyzers, providing realistic information about the current state of the art of the technology.

### Hydrogen storage

As already said, P2P is an energy storage technology with the main advantage to rely on an energy carrier as energy storage medium. This means that hydrogen can be stored in different ways and for as long as it is required, as opposed to other technologies which cannot be used for long-term energy storage. Nevertheless, despite this flexibility, the term-period for which hydrogen energy storage is most attractive is in the order of days to months. For shorter or longer storage periods, other technologies exhibit a better trade-off between discharge time and efficiency of storage [6].

Hydrogen is known to be the fuel with the highest gravimetric density but with the main shortcoming of having one of the lowest densities. Hence, different storage strategies are

**Table 3 – Commercial availability of electrolyzers.**

| Type  | Label | OEM                           | Model          | $P_{out}$ [bar] | $H_2$ Yield [ $Nm^3/h$ ] | SEC [kWh/kg $H_2$ ]                   |
|-------|-------|-------------------------------|----------------|-----------------|--------------------------|---------------------------------------|
| AEC   | A1    | SunFire [44]                  | HYLINK         | 30              | 1090                     | 52.3                                  |
|       | A2    | Enapter [45]                  | EL 2.1         | 35              | 0.5                      | 53.4                                  |
|       | A3    | Green Hydrogen [46]           | A30            | 35              | 30                       | 52.2                                  |
|       | A4    |                               | A60            |                 | 60                       | 52.2                                  |
|       | A5    |                               | A90            |                 | 90                       | 53.6                                  |
|       | A6    | McPhy [47]                    | Baby           | 1               | 0.4                      | 83.5                                  |
|       | A7    |                               | P              | 1–2.5           | 0.5–0.8                  | 66.8–62.6                             |
|       | A8    |                               | M              | 1–2.5           | 2.4–4.4                  | 64.9–65.7                             |
|       | A9    |                               | H              | 4–8             | 3–10                     | 66.7                                  |
|       | A10   |                               | McLyzer 10-30  | 30              | 10                       | 55.6                                  |
|       | A11   |                               | McLyzer 20-30  |                 | 20                       |                                       |
|       | A12   |                               | McLyzer 100-30 |                 | 100                      |                                       |
|       | A13   |                               | McLyzer 200-30 |                 | 200                      |                                       |
|       | A14   |                               | McLyzer 400-30 |                 | 400                      |                                       |
|       | A15   |                               | McLyzer 800-30 |                 | 800                      |                                       |
|       | A16   | Nel Hydrogen [48]             | A150           | 1–200           | 50–150                   | 42.3 <sup>a</sup> - 49.0 <sup>a</sup> |
|       | A17   |                               | A300           |                 | 150–300                  |                                       |
|       | A18   |                               | A485           |                 | 300–485                  |                                       |
|       | A19   |                               | A1000          |                 | 600–970                  |                                       |
|       | A20   |                               | A3880          |                 | 2400–3880                |                                       |
| PEMEC | A21   | Nel Hydrogen [48]             | S10            | 13.8            | 0.27                     | 67.9                                  |
|       | A22   |                               | S20            |                 | 0.53                     |                                       |
|       | A23   |                               | S40            |                 | 1.05                     |                                       |
|       | A24   |                               | H2             | 15–30           | 2                        | 81.2                                  |
|       | A25   |                               | H4             |                 | 4                        | 77.9                                  |
|       | A26   |                               | H6             |                 | 6                        | 75.7                                  |
|       | A27   |                               | C10            |                 | 10                       | 69.0                                  |
|       | A28   |                               | C20            |                 | 20                       | 66.8                                  |
|       | A29   |                               | C30            |                 | 30                       | 64.5                                  |
|       | A30   |                               | M100           | 30              | 103                      | 50.4 <sup>a</sup>                     |
|       | A31   |                               | M200           |                 | 207                      |                                       |
|       | A32   |                               | M400           |                 | 413                      |                                       |
|       | A33   |                               | M4000          |                 | 4000                     |                                       |
|       | A34   | ITM Power [49]                | HGAS1SP        | 20              | 0.99                     | 63.6                                  |
|       | A35   |                               | HGAS2SP        |                 | 1.98                     | 63.2                                  |
|       | A36   |                               | HGAS3SP        |                 | 3.24                     | 65.3                                  |
|       | A37   |                               | HGASXMW        |                 | 15.17                    | 59.7                                  |
|       | A38   | Hydrogenics <sup>b</sup> [49] | HyLYZER 300    | 30              | 300                      | 53.4                                  |
|       | A39   |                               | HyLYZER 1000   |                 | 1000                     |                                       |
|       | A40   |                               | HyLYZER 5000   |                 | 5000                     |                                       |
| SOEC  | A41   | SunFire [44]                  | HYLINK         | 1               | 750                      | 40.0                                  |

<sup>a</sup> Power consumption provided by manufacturer accounts for the stack only and not for the BoP.

<sup>b</sup> Hydrogenics has been acquired by Cummins.

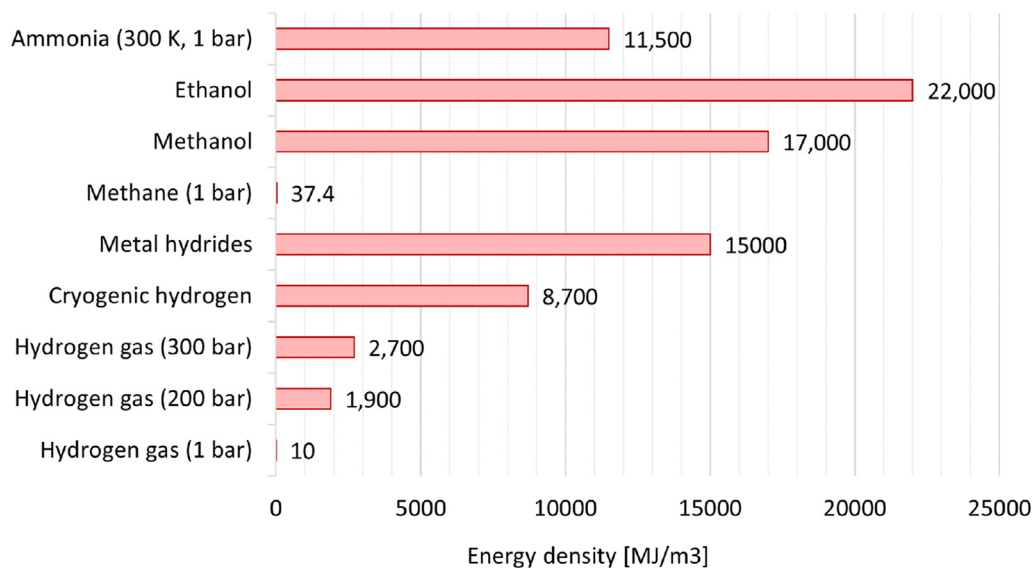


Fig. 3 – Energy density of different fuels. Adapted from Ref. [38].

applied to overcome the low density of hydrogen, be it in gaseous, liquid or solid states; for instance, it is common to liquefy hydrogen through compression with the objective to attain a higher density, but this is very energy intensive. As a representation of this, Fig. 3 shows the energy densities of hydrogen (at different pressures) and other fuels also used for energy storage. It is observed that the energy density of hydrogen at ambient conditions is much lower than that of other gases (e.g., methane, ethane), liquids (e.g., methanol) or solids (e.g., ammonia); moreover, even if the storage pressure of hydrogen were increased to values as high as 300 bar, the energy density would still be significantly lower. Only liquid (cryogenic) or solid (metal hydrides) storage would make a difference but these processes are either highly energy intensive or not suitable for large-scale hydrogen storage.

Other substances with higher energy densities, such as ammonia or syn-gas, can be produced using hydrogen as feedstock. This facilitates transportation but incurs higher energy losses due to the incorporation of an additional process where large amounts of energy are consumed (either as heat, mechanical power or both). For instance, the FLEXn-CONFU project (acronym standing for *Flexibilize combined cycle power plant through power-to-X solutions using non-conventional fuels*) funded by the European Commission studies the use of ammonia as a way to transport hydrogen and produce power [21], a solution that is beneficial to transport large amounts of energy over long distances. This concept falls beyond the scope of this study though, as reported in Section [Hydrogen distribution](#), and hence the conversion of hydrogen into other substances (fuels) is left out of the analysis.

#### Compressed hydrogen gas

Hydrogen compression is the most common means to store and distribute hydrogen in relatively small quantities, 5–10 kg<sub>H<sub>2</sub></sub>/tank. The pressure at which hydrogen is compressed depends on the application and it ranges from 50 to 400 bar for stationary applications and to 900 bar for mobility

applications (where high density is a critical requirement). This implies large pressure ratios (typically higher than 30:1), enabled by volumetric machines such as reciprocating or diaphragm compressors.

Diaphragm compressors compress small to medium flow rates of hydrogen efficiently, attaining high to extremely high pressure ratios of more than 5000:1 [50]. The operating principle of diaphragm compressors ensures oil and leakage free compression with high purity of the outlet flow. However, when operation is discontinuous (frequent start/stop), the lifetime of the diaphragm can decrease substantially, which means more frequent servicing and, therefore, higher maintenance costs. In applications with more frequent transient and/or discontinuous operation, hydraulically-driven dry-running reciprocating compressors are a viable alternative. They also enable high delivery pressures of up to 3000 bar [50] with also oil, leakage and technically abrasion free compression. With this in mind and given the intermittent nature of RES for the production of green energy (wind and solar photovoltaic are the dominant sources of renewable energy, in addition to hydro), reciprocating compressors with several stages of intercooling are deemed the best solution for hydrogen compression in this work.

Delivery pressure from the electrolyser is a key parameter determining compressor power during the downstream compression of H<sub>2</sub> for storage, since this is the pressure (same for temperature) at the intake of the storage compressor. This effect is assessed in Fig. 4a, showing that compression from 1 to 1000 bar requires twice as much work as compression from 30 to 1000 bar, 4 kWh/kg<sub>H<sub>2</sub></sub> and 2 kWh/kg<sub>H<sub>2</sub></sub> respectively.

Compression work is influenced not only by inlet conditions and outlet pressure but also by compressor type and, linked to this, how the compression process is carried out. Fig. 4a shows the differences between isentropic (reversible and adiabatic) and reversible, intercooled compressions, the latter of which resembles an isothermal compression process. The different nature of these processes is reflected in



the value of the polytropic index  $k$  in Eq. (12), yielding compression work. When  $k = 1$ , compression is at constant temperature. When  $k$  equals the ratio of specific heats  $\gamma$  ( $\gamma = C_p/C_v$ ), which is 1.41 for hydrogen, compression is isentropic and compression work increases with respect to the isothermal case. For adiabatic compressors not working reversibly,  $k > \gamma$ . Interestingly, volumetric compressors like diaphragm and reciprocating are cooled internally but this does not enable isothermal compression. In practice,  $1 < k < \gamma$  and the exact value of  $k$  is determined experimentally.

Fig. 4a provides an estimate of compression work with and without intercooling between stages. This information is complemented by Table 4 which shows the resulting polytropic index  $k$  for different arrangements of the compression system. Two cases are considered. Case 1 considers individual isentropic compression stages with intermediate cooling; for each individual compression stage,  $k = \gamma = 1.41$ . Case 2 considers that each compression stage is adiabatic but not reversible, hence  $k > \gamma = 1.41$ . Two conclusions are drawn from the table:

- Increasing the number of stages brings about a reduction of compression work because the compression process becomes closer to isothermal.
- For a given number of stages, non-isentropic compression by the individual stages increases the total work needed to compress hydrogen.

In addition to these two conclusions, it must also be noted that a higher number of stages implies higher capital costs. Also, departing from isentropic (i.e. lower efficiency of the individual compression stages) poses a higher demand on the interstage cooling system (coolant pump) because of the higher inlet temperature to the intercooler.

That said, and for the purpose of defining the compression energy requirements for the different scenarios in Table 5, pressure ratio per compression stage is calculated according to the next guidelines [51]:

1. Maximum pressure ratio per stage is 4:1.
2. Maximum outlet temperature for all stages is 420 K. Controlling that this temperature does not exceed this upper limit can be achieved either by decreasing inlet gas temperature (more intense cooling) or by increasing stage count.

Hence, the number of compression stages ( $n_{\text{stages}}$ ) and compressor work ( $W_{\text{compressor}}$ ) can be estimated from Eqs. (11) and (12).

$$n_{\text{stage}} = \frac{\log \frac{P_2}{P_1}}{\log \text{PR}_{\text{stage}}} \quad (11)$$

$$W_{\text{compressor}} = \dot{m}_{\text{H}_2} \cdot \sum_{i=1}^{n_{\text{stages}}} \frac{\frac{k}{k-1} \cdot R \cdot T_{1,i} \cdot Z_i \cdot \text{PR}_i^{\frac{k-1}{k}} - 1}{\eta_{\text{compressor}}} \quad [\text{W}] \quad (12)$$

where:

- $\dot{m}_{\text{H}_2}$  is the mass flow rate of hydrogen [kg/s].

- $P_1$  and  $P_2$  are the inlet and outlet pressures of the compressor [bar].
- $\text{PR}_i$  is the stage pressure ratio for each compression stage.
- $k$  is the polytropic index of the gas.
- $R$  is the universal gas constant for  $\text{H}_2$ ,  $4124 \text{ J kg}^{-1} \text{ K}^{-1}$ .
- $T_i$  is the fluid inlet temperature for each compression stage.
- $Z_i$  is the compressibility factor for each compression stage. Values of the compressibility factor of hydrogen can be found at [52].
- $\eta_{\text{compressor}}$  is the efficiency of the compressor.

In addition to the specific work of the compressor, the work needed to drive the cooling water pump of the intercooler must also be calculated in order to obtain the total power consumption of the hydrogen compression system. Fig. 4b shows the assumptions made to obtain these performance indicators, which can be estimated with the equations below:

$$\dot{m}_{\text{H}_2\text{O}} = \frac{\dot{m}_{\text{H}_2} (h_{1\text{H}_2} - h_{2\text{H}_2})}{h_{2\text{H}_2\text{O}} - h_{1\text{H}_2\text{O}}} \quad [\text{kg s}^{-1}] \quad (13)$$

$$W_{\text{pump}} = \sum_{i=1}^{n_{\text{stages}}} \frac{g \cdot H_i \cdot \dot{m}_{i,\text{H}_2\text{O}}}{\eta_{\text{pump}}} \quad [\text{W}] \quad (14)$$

where:

- $h$  refers to the specific enthalpy of  $\text{H}_2\text{O}$  and  $\text{H}_2$  at the inlet (1) and outlet (2) of/from the intercooler [ $\text{kJ kg}^{-1}$ ].
- $\dot{m}_{i,\text{H}_2}$  and  $\dot{m}_{i,\text{H}_2\text{O}}$  are the corresponding mass flow rates [ $\text{kg s}^{-1}$ ] for hydrogen and water for each of the intercooling stages.
- $g$  is the gravitational acceleration, estimated at  $9.81 \text{ [m s}^{-2}]$ .
- $H_i$  is the head of the pump [m] for each of the intercooling stages.
- $\eta_{\text{pump}}$  is the efficiency of the pump [%].
- The pressure ratio between the hot (hydrogen) and cold (water) sides of the heat exchangers is set to 10. Therefore, pressure on the hydrogen side is ten times higher than on the water side. This assumption is considered when calculating the pump head for each intercooling system.

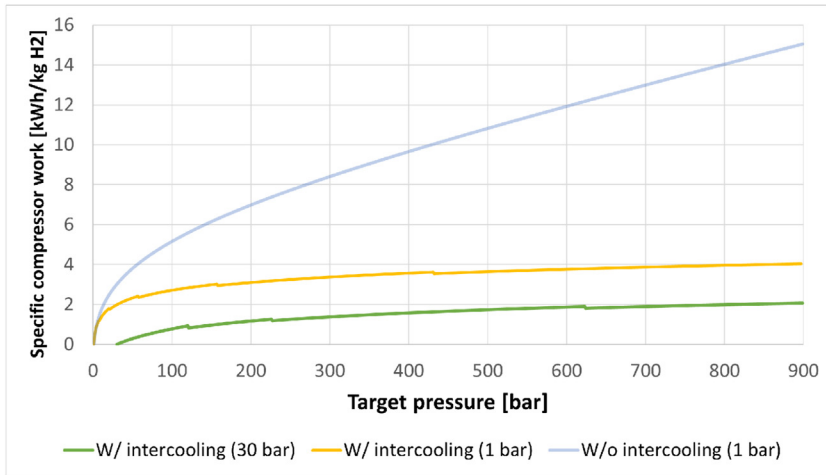
Table 5 shows the power demand of the compression system for different cases, based on the calculations in Eqs. (12) and (14).

#### Liquefied hydrogen ( $\text{LH}_2$ )

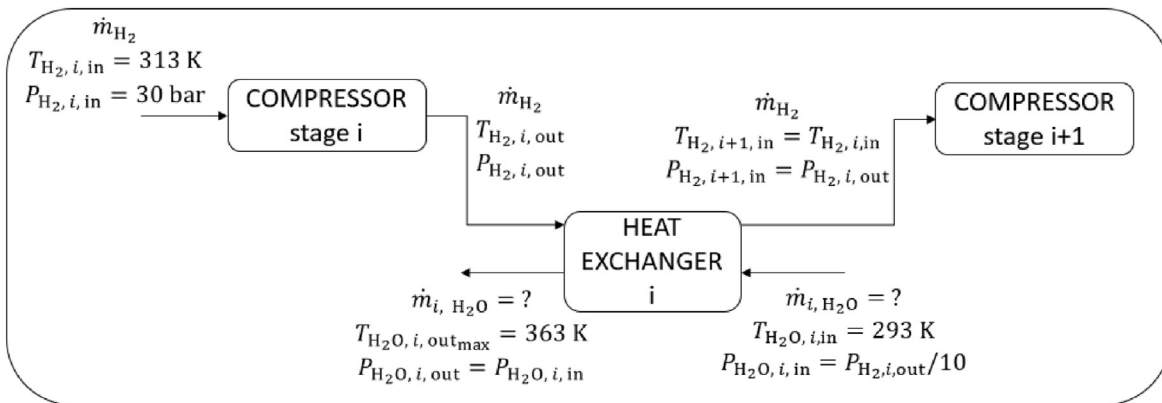
Hydrogen is commonly produced at close to ambient pressure and temperature, in the range from 1 to 30 bar and from 303 to 333 K, as stated in section Hydrogen production. Nevertheless, in this pressure range, hydrogen is found in the liquid state only at temperatures below 20.37 K (1 bar) to 33.14 K (12.79 bar - critical pressure) [54]. Therefore, a cryogenic plant is needed in order to reduce the temperature of hydrogen to such extremely low values if  $\text{H}_2$  is to be stored in liquid state. Fig. 5 shows a generic layout of a facility to liquefy hydrogen.

Liquefaction of hydrogen can be divided into four general stages:

1. Precompression (at ambient conditions).
2. Precooling (ambient to about 80 K).



(a) Hydrogen compression work. In brackets, operating pressure of the electrolyser.



(b) Operating conditions of the H<sub>2</sub>/H<sub>2</sub>O intercooler between compression stages. Mass flow rate of cooling water depends on inlet temperature and pressure ratio of the upstream compression stage.

**Fig. 4 – Power consumption and operating conditions of the compression system.**

3. Cryo-cooling (80 K–30 K).
4. Liquefaction (30 K to LH<sub>2</sub> at atmospheric pressure).

Losses along the LH<sub>2</sub> pathway are intrinsic to the utilisation of a cryogenic fluid. They occur when hydrogen in these conditions is transferred between two vessels (liquefaction plant to tank-truck, tank-truck to storage station, storage station to end-user through a pump or compressor, and eventually final use in a fuel cell or other power generation device) and when the fluid is warmed up due to heat transfer from the environment [56]. Nevertheless, in spite of the highly energy intensive processes and the need for more auxiliary equipment to keep hydrogen stored in these conditions, the much higher energy and mass density is a clear, direct benefit of dealing with cryogenic hydrogen: 0.083 kg/m<sup>3</sup> at 1.013 bar and 295 K as opposed to 76.2 kg/m<sup>3</sup> at the same pressure but 15 K [54].

Within the scope of this work, a research study has been carried out to screen the different liquefaction plant concepts proposed in the public domain. Some of these plants have been constructed whilst others are still in the conceptual stage. The aim of this assessment is to gather actual, reliable information about cryogenic hydrogen-liquefaction plants which can be used to estimate the power consumption in these facilities. IDEALHY is a very interesting hydrogen-liquefaction project funded by the European Commission and completed in 2013 [57]. The results from this project showed that a total power consumption of around 6.7 kWh/kg<sub>H<sub>2</sub></sub> ( $\approx 20\%$  of H<sub>2</sub> LHV) could be achieved, which is around half of what had been declared for existing H<sub>2</sub> liquefaction plants [58]. Furthermore, recent investigations have shown that further optimisation of the concept would enable an even lower power requirement of approximately 5.9 kWh/kg<sub>H<sub>2</sub></sub> [59,60].

**Table 4 – Calculation of the global polytropic index of the (complete) compression system with intercooling. Isentropic compression of each stage is considered in Scenario 1 ( $k_i = 1.41$ ) whereas Scenario 2 considers adiabatic, irreversible compressions with  $k_i = 1.52$  (this corresponds to a polytropic efficiency of around 85%). Compressor inlet temperature is set to 298.15 K for all stages.**

|                | Polytropic Index<br>( $k_{\text{compression}}$ ) | Scenarios    |              |
|----------------|--|--------------|--------------|
|                |  | $k_i = 1.41$ | $k_i = 1.52$ |
| Pressure Ratio | 10 (2 compression stages)                        | 1.1693       | 1.2055       |
|                | 100 (4 compression stages)                       | 1.0781       | 1.0932       |
|                | 1000 (6 compression stages)                      | 1.0512       | 1.0608       |

**Table 5 – Power demand of H<sub>2</sub> compression in different scenarios.**

| Label | $T_1$<br>[K] | $P_1$<br>[bar] | $\eta_{\text{compressor}}/\eta_{\text{pump}}$<br>[%] | $n_{\text{stages}}^a$<br>[–] | $P_{\text{tank}}$<br>[bar] | $w_{\text{total}}$<br>[kWh/kg H <sub>2</sub> ] |
|-------|--------------|----------------|--|------------------------------|----------------------------|--|
| B1    | 313          | 30             | 70 [53]/90   | 1                            | 50                         | 0.29   |
| B2    |              |                |  | 3                            | 350                        | 1.48   |
| B3    |              |                |  |                              | 500                        | 1.73   |
| B4    |              |                |  | 4                            | 700                        | 1.89   |
| B5    |              |                |  |                              | 900                        | 2.07   |

<sup>a</sup> The temperature of hydrogen at the outlet from the intercooler is set to  $T_1$  for all stages.

A summary of the most relevant studies of H<sub>2</sub> liquefaction plants in the last decades is shown in Table 6. Amongst these, two reference plants will be considered in the analysis to estimate round-trip efficiency presented in Section Analysis: one plant already in operation and one state-of-art LH<sub>2</sub> plant concept.

The power requirements for liquefaction of hydrogen are high, as reported in Table 6. Nevertheless, energy recovery strategies from the different processes involved might help reduce the power consumption elsewhere in the system concept considered in this study. For instance, Voth and Parrish deal with different systems to recover energy from a hydrogen liquefaction plant, stating that up to 60% of the ideal power could be recovered depending on the desired outlet pressure [69]. Furthermore, Calabrese et al. also deal with different strategies to recover energy but, in this case, from a natural gas liquefaction process [70]. In contrast to these works though, the present study does not aim at optimising the integration of all systems but, on the contrary, it only considers the hydrogen liquefaction options that are (or might be) commercially available. In this regard, the conclusions of the analysis could be deemed conservative given that waste heat recovery is not considered.

#### Metal hydrides (MH)

The combination of metals or alloys with hydrogen leads to the formation of new compounds termed *metal hydrides*. These new compounds are characterised by a higher density, exceeding 115 kgH<sub>2</sub>/m<sup>3</sup> (Fig. 3). However, their gravimetric density is low and the weight percentage of H<sub>2</sub> (wt%) is  $\approx$  7%

only. More information about recent progress made in this area can be found in the reference list [71].

Hydrogen loading and unloading are chemical reactions when hydrogen is stored in the form of metal hydrides. As such, these processes are influenced by thermodynamic and kinetic aspects mostly [72]. During loading, hydrogen is adsorbed through an exothermic reaction. Conversely, hydrogen is released (desorbed) when heat is supplied to the metal hydride. This process is described by Eq. (15), where  $M_e$  refers to a specific metal:



The particular composition of the metal hydride considered determines the amount of heat exchanged during adsorption/desorption to load/unload hydrogen. Accordingly, many of the challenges in using such materials are related to the thermodynamics and kinetics of dehydrogenation, which determine the hydrogen discharge rate and the heat supply needed to enable efficient hydrogen desorption from the metal hydride. More information about these two processes as well as about metal hydrides in general can be found in the public domain [73–75].

Research has been conducted to find the different options available when considering metal hydrides for H<sub>2</sub> storage. These options are typically characterised by low release rates but this can be solved if an array of multiple systems is adopted. Table 7 shows some options available in the market.

As highlighted previously, the adsorption/desorption processes make use of cooling and heating sources. These reservoirs are at temperatures of  $\sim$ 10°C for cooling and  $\sim$ 50°C for heating, even though this depends on the specific MH chosen. In this study, it is considered that these cooling/heating sources are available from waste heat streams and that there is no need for additional electric power consumption. Hence, the figure of merit used in this study, round-trip efficiency, is not influenced by this effect.

#### Hydrogen distribution

Hydrogen production can be implemented through either decentralised or centralised paradigms. In the former case, smaller hydrogen production plants are installed closer to the end-consumer whereas, in the latter, a large facility supplies hydrogen to a community of consumers who may be distant from one another. Having on-site hydrogen production (i.e., decentralised) results in a higher round-trip efficiency of the P2P concept since distribution to the end-user does not add significant energy losses. In addition, if compressed H<sub>2</sub> is used for storage, very high storage pressures are typically not needed and this saves both capital costs (less costly storage tanks) and auxiliary power consumption. However, there are also financial advantages to having a centralised hydrogen production scheme as this enables the exploitation of economies of scale both for the capital and operational costs.

Fig. 6 shows the layout of consumption nodes that is considered in this work. There are five nodes at an average distance of 25 km from one another. Additionally, the first and last nodes are 50 km from the production facility, what

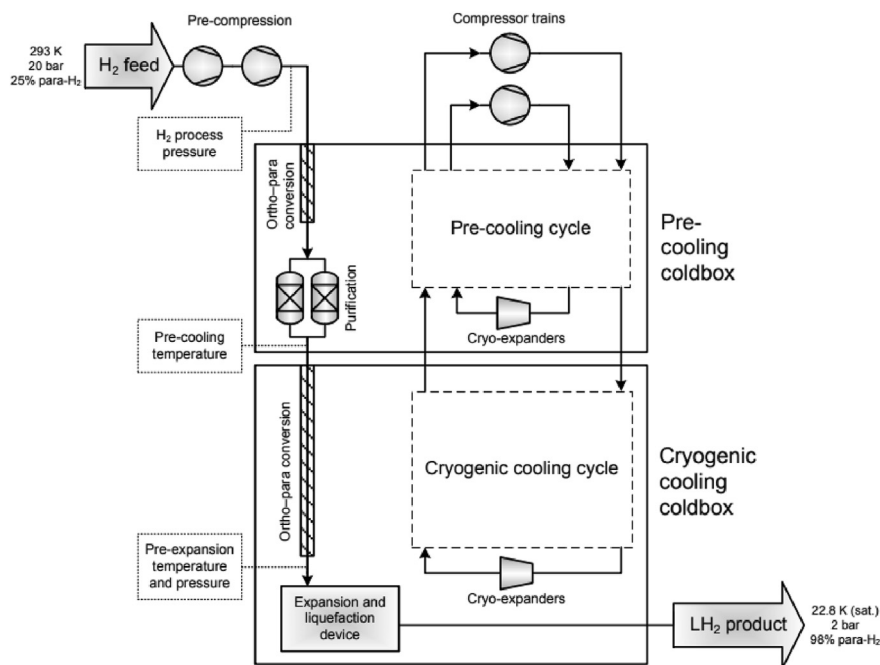


**Fig. 5 – Simplified process flow diagram of a hydrogen liquefaction plant [55]. (Copyright © IIF/IIR. Published with permission of the International Institute of Refrigeration (IIR)).**

translates into a total distance travelled of around 200 km per trip. The option of choice for distribution is a Fuel Cell Electric Truck (FCET), therefore running on hydrogen fuel [79], due to its versatility to distribute hydrogen in different mass states and the relatively low cost compared to, for instance, hydrogen-pipelines. Additionally, the latter would only be cost effective for the case of transporting large amounts of compressed- $H_2$ . Hence, tank-trucks are the preferred option for hydrogen distribution in this paper.

This means that there are two contributions to the total energy requirement for  $H_2$  distribution: i) power consumed by the electrolyser to produce the amount of hydrogen consumed by the FCET; and ii) power consumed for the compression to 900 bar to enable the filling of the tank. Table 8 shows the power required to distribute hydrogen in different states with a FCET, as reported in section [Hydrogen storage](#).

### Hydrogen consumption

There are several applications where an energy carrier such as hydrogen can be used: mobility, feedstock, power generation, and others [10,13,17,37,38]. Nevertheless, in this work, only power generation is considered in order to provide more focused conclusions about the feasibility and interest of power-to-power applications.

Fuel Cells (FC) are usually recognised as the most interesting technology to produce power from hydrogen [82]. Nonetheless, with the recent interest triggered by hydrogen technologies to decarbonise many sectors (see Section [Introduction](#)), other power technologies are being upgraded to enable the direct utilisation of hydrogen as main fuel. Gas Turbines (GT) are one of the technologies that is catching up more quickly with FCs, thanks to the lessons learned from

**Table 6 – Existing hydrogen liquefaction plants and studies.**

| Label | $P_1$<br>[bar] | $T_{final}$<br>[K] | $P_{final}$<br>[bar] | Power requirement<br>[kWh/kg $H_2$ ] | Year | Ref.    | Built/Study |       |
|-------|----------------|--------------------|----------------------|--------------------------------------|------|---------|-------------|-------|
| B6    | 1.01           | 20.57              | 9.29                 | 10.85                                | 1978 | [61]    | Study       |       |
| B7    | 1.06           | 20.45              | 1.06                 | 8.53                                 | 1997 | [62]    |             |       |
| B8    | 1.06           | 20.45              | 1.06                 | 8.69                                 | 1997 | [62]    |             |       |
| B9    | 1.06           | 20.45              | 1.06                 | 8.58                                 | 1997 | [62]    |             |       |
| B10   | 1.00           | 20.20              | 1.00                 | 6.93                                 | 2001 | [63]    |             |       |
| B11   | 1.01           | 20.40              | 1.06                 | 8.72                                 | 2004 | [64]    |             |       |
| B12   | 1.00           | 20.00              | 1.00                 | 8.73                                 | 2008 | [65]    |             |       |
| B13   | 60.00          | 20.00              | 1.50                 | 5.29                                 | 2008 | [66]    |             |       |
| B14   | 21.00          | 20.20              | 1.00                 | 6.35                                 | 2010 | [67]    |             |       |
| B15   | 25.00          | 22.80              | 2.00                 | 6.00                                 | 2017 | [60,59] |             |       |
| B16   | 25.00          | 22.80              | 2.00                 | 6.30                                 | 2017 | [60,59] |             |       |
| B17   | 21.00          | 21.00              | 1.30                 | 13.60                                | 1992 | [68]    |             | Built |
| B18   | 24.00          | 21.00              | 1.30                 | 11.90                                | 2007 | [58]    |             |       |

**Table 7 – Market availability of hydrogen storage solutions based on metal hydrides.**

| Label | Manufacturer               | Model                   | Capacity [Nm <sup>3</sup> ] | System Mass [kg] | P <sub>charge</sub> [bar] | P <sub>discharge</sub> [bar] | H <sub>2</sub> discharge rate [Nm <sup>3</sup> /h] |
|-------|----------------------------|-------------------------|-----------------------------|------------------|---------------------------|------------------------------|--|
| B19   | HBank [76]                 | HB-SS-3300              | 3.3                         | 37               | 4–5                       | > 0.1 ≤ 2.0                  | ≤10 (25°C)   |
| B20   |                            | HB-SS-16500             | 16.5                        | 190              | (25°C)                    | (25°C)                       | ≤50 (25°C)   |
| B21   | Pragma Industries [77]     | MH 7000he <sup>a</sup>  | 7.0                         | 90               | –                         | 10 to 1                      | 6.6  |
| B22   |                            | MH 10000he <sup>a</sup> | 10.0                        | 115              |                           |                              | 9  |
| B23   | h2planet <sup>b</sup> [78] | MyH2 7000               | 7.0                         | 47               | ≤30                       | ≤30                          | 2 (25°C)   |

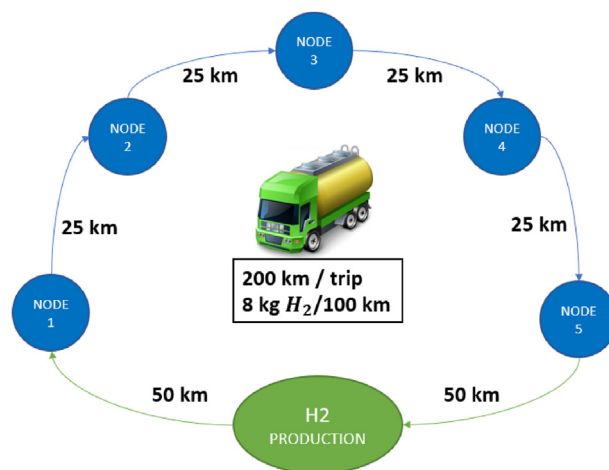
<sup>a</sup> Cooling water is needed. No more data provided by manufacturer.  
<sup>b</sup> Personal communication with h2planet.

hydrogen co-firing in the last decades [83–86]. However, challenges for a flexible and interrupted operation with 100% hydrogen combustion still remain; an overview of the state-of-art of hydrogen operation of GTs is available in a recent report by the European Turbine Network [87]. As mentioned in Section Introduction, the HYFLEXPOWER and ROBINSON projects deal with the design and operation of the first 100% H<sub>2</sub> GT and mGT in Europe. In an industrial context, a representative of Siemens Energy reported recently that, in addition to developing new technologies to enable 100% H<sub>2</sub> operation, “all the technology solutions they are working on can be retrofitted to adapt its existing fleet of GTs for operation on hydrogen fuel” [88], hence reducing the time frame to achieve carbon neutrality of the power sector.

This paper is focused on micro Gas Turbines (mGT) rather than larger gas turbines (≤500kWe). These smaller engines exhibit two main differences with respect to the larger units, brought about by the need to use radial machinery as a consequence of the low volumetric flow rate of air through the engine (compressor and expander). Indeed, the utilisation of single stage radial compressors limits the pressure ratio of the engine to values lower than 4 (approximately) and the lack of internal cooling systems built into radial expanders limits turbine inlet temperature to values not higher than 950°C. These key design parameters are in contrast with pressure ratios (≈20–25) and combustor outlet temperatures (1500–1600°C) commonly found in heavy-duty gas turbines. As a consequence of this, mGTs typically rely on recuperative cycle layouts to attain higher thermal efficiency and they also need specific combustor designs to enable operation on 100% H<sub>2</sub>, even though this can largely leverage on the experience gained with larger engines. As far as this work is concerned, only mGTs burning 100% H<sub>2</sub> are considered, even if this capability is not offered by any commercial product in the market yet, as shown in Table 9.

## Analysis

The processes involved in power-to-power energy storage solutions have been discussed in Section Power-to-hydrogen-to-power: production, storage, distribution and consumption. The aim of this section is to estimate the round-trip efficiency of micro power-to-power energy storage solutions using micro-gas turbines, shown schematically in Fig. 1.

**Fig. 6 – Centralised H<sub>2</sub> distribution layout using a Fuel Cell Electric Truck (FCET).**

The process of storing energy to deliver it at a later time does not come without losses given that the different energy conversion steps involved are irreversible, or just because there is auxiliary equipment that consumes part of the energy taken from the grid (or produced by the primary power generation system). The ratio of the energy delivered back to the user (or the grid) to that taken from the primary source of electricity (in the context of this work) is termed round-trip efficiency and is typically expressed as follows, where  $E$  stands for electric energy:

$$\eta_{\text{round-trip}} = \frac{E_{\text{out}}}{E_{\text{in}}} \quad (16)$$

For the micro power-to-power energy storage considered in this work, electric power produced by a photovoltaic power station  $E_{\text{in}}$  is converted into hydrogen through water electrolysis (Table 3); this means that the system proposed classifies as chemical energy storage. Power is consumed to operate the electrolyser and it is also needed for the downstream processing of the hydrogen produced, be it for high-pressure gaseous storage (Table 5), liquefied H<sub>2</sub> storage (Table 6) or to load/unload metal hydrides (Table 7). The amount of H<sub>2</sub> consumed by FCETs for distribution can also be expressed in terms of equivalent auxiliary power consumption (Table 8). Eventually, when electricity is demanded by the grid or directly by a consumer, the hydrogen stored is

**Table 8 – Hydrogen transportation/distribution options using a Fuel Cell Electric Truck (FCET).**

| Label | H <sub>2</sub> State |         |       | FCET Consump.<br>[kg H <sub>2</sub> /100 km] | Capacity<br>[kg <sub>H<sub>2</sub></sub> /truck] | Spec. fuel consump. <sup>c</sup> [200 km]<br>[kg <sub>H<sub>2</sub></sub> , consumed/kg <sub>H<sub>2</sub></sub> , transported] |
|-------|----------------------|---------|-------|--|--|---|
|       | State                | P [bar] | T [K] |  |  |   |
| C1    | Gas                  | 300     | 288   | 8 [79]                                       | 605 <sup>a</sup>                                 | 0.0279  |
| C2    | Gas                  | 517     | 288   |  | 1135 <sup>a</sup>                                | 0.0141  |
| C3    | Liquefied            | 2       | 15    |  | 3815 <sup>b</sup>                                | 0.0042  |
| C4    | Solid                | –       | –     |  | 900 [80]   | 0.0178  |

<sup>a</sup> Capacity is calculated considering a storage volume available of 26.9 m<sup>3</sup> (Type-II gas cylinder) and 34.7 m<sup>3</sup> (Type-IV gas cylinder) for the cases of gaseous storage at 300 bar and 517 bar respectively. Personal communication with Calvera [81].

<sup>b</sup> Capacity is calculated considering a storage volume available of 50.0 m<sup>3</sup>.

<sup>c</sup> Specific power consumption for distribution under different scenarios can be calculated using the specific fuel consumption reported.

converted into electric power and heat by a micro gas turbine (Table 9).

In order to avoid dealing with a large number of theoretically-feasible solutions, the analysis in this paper is limited to the possible combinations of 1) three electrolyser technologies, 2) three H<sub>2</sub> storage states and 3) one mGT option. This yields a total of nine micro power-to-power energy storage combinations to be explored:

1. Production: A1 (AEC), A39 (PEMEC) and A41 (SOEC).
2. Storage and distribution: B3–C2 (gas compressed at 500 bar), B15–C3 (liquefied-H<sub>2</sub>), B20–C4 (metal hydride).
3. Power generation: D3 (mGT).

Fig. 7 shows the energy balance of the power-to-power solutions listed above. On the horizontal scale, the micro gas turbine produces positive power whereas the power produced by remainder components is negative (i.e., power consumption rather than generation). As expected, the electrolyser holds the largest share of energy consumption, ranging from 86 to 98% of the total flow of energy into the system (power produced by the micro gas turbine), and storage and distribution fall well behind. For the compressed-H<sub>2</sub> cases, the energy consumed to drive the compressors more than doubles that needed for distribution, 3.5% and 1.5% of the total consumption of energy. For liquefied-H<sub>2</sub> storage, liquefaction stems as a highly energy intensive process but, on the other hand, it provides a much higher energy density; i.e., much more energy is transported in each trip (see Table 8). As a result, storage accounts for 10%–13% of the total energy consumption whereas distribution takes 0.4% of the total energy in only. The case of MH is different to the other two

storage options since storage is almost free energy-wise, if and where there is a heat source available at a suitable temperature or when the metal hydride is suitable for operation at ambient temperature (see Section Metal Hydrides (MH)). Therefore, storage is considered energy-neutral and distribution takes 2% of the total energy in.

A closer look into the energy consumed by the electrolyser in each case, Fig. 7, reveals that this energy consumption is largely reduced when SOECs are used as opposed to either AEC or PEMEC: 40 kWh/kg<sub>H<sub>2</sub></sub> against 52 kWh/kg<sub>H<sub>2</sub></sub> and 53 kWh/kg<sub>H<sub>2</sub></sub> respectively. This difference comes about because of the working temperature, as explained in Section Hydrogen production, and implies that a higher grade heat source which can both raise the temperature of and evaporate the inlet water stream is needed in order to operate the SOEC at the rated conditions. Otherwise, a boiler burning H<sub>2</sub> could be used but this would be at the cost of reducing electrolyser efficiency and of adding more capital cost to the system. Therefore, despite the fact that solid oxide electrolysers can be operated reversibly as solid oxide fuel cells, thus reuniting hydrogen and power generation into one single device, this option is left out of the scope of this work due to the lower technology readiness level of such systems and to the lack of a high grade (waste) energy source available.

A conceptual scheme of the power-to-power system considered in this work is presented in Fig. 8. Based on this and on the energy balance shown in Fig. 7, the round-trip efficiency of the system can be calculated with Eq. (16). This information ( $\eta_{\text{round-trip}}$ ) is reported in Fig. 9 for the cases under consideration, showing values ranging from 20% to 29% depending on the configuration of choice. According to the foregoing discussion in this section, the primary drivers of

**Table 9 – Commercially available micro-gas turbines (efficiency referred to LHV).**

| Label | Manufacturer         | Model              | Fuel Consump.<br>[kg <sub>H<sub>2</sub></sub> /h] | Rated<br>Power [kWe] | Spec. Rated<br>Power [kWe/kg <sub>H<sub>2</sub></sub> ] | $\eta_e$<br>[%] |
|-------|----------------------|--------------------|---|----------------------|---|-----------------|
| D1    | Capstone [89]        | C30                | 3.22  | 30                   | 9.32  | 28.0            |
| D2    |                      | C65                | 6.25  | 65                   | 10.39   | 31.2            |
| D3    |                      | C200s <sup>a</sup> | 16.90   | 200                  | 11.83   | 35.5            |
| D4    | Flex Energy [90]     | GT333s             | 30.77   | 333                  | 10.82   | 32.5            |
| D5    | Ansaldo Energia [91] | AE-T100            | 9.99  | 100                  | 10.01   | 30.0            |
| D6    | Aurelia [92]         | A400               | 29.85   | 400                  | 13.40   | 40.2            |
| D7    | MTT [93]             | EnerTwin           | 0.60  | 3.2                  | 5.33  | 16.0            |

<sup>a</sup> Capstone C600s, C800s and C1000s packages are arrays of 3, 4 and 5C200s units respectively.

round-trip efficiency are the power consumption of the electrolyser and the thermo-mechanical energy conversion process in the micro gas turbine; yet, given that the mGT specifications are the same for all cases, the variations of round-trip efficiency from one case to another in Fig. 9 are brought about solely by the electrolyser technology used (AEC, PEMEC or SOEC). For cases based on SOEC, the highest efficiency is obtained when hydrogen is stored in the form of MH ( $\approx 29.0\%$ ), followed closely by compressed- $H_2$  ( $\approx 27.9\%$ ), and  $LH_2$  at a further distance ( $\approx 25.6\%$ ). This latter value is obtained when one of the lowest specific power requirement of the  $LH_2$  plant is chosen from the options in Table 6, even though, interestingly, this is not the minimum value (B18). Actually, if the value corresponding to one of the existing  $LH_2$  plants were selected (for instance,  $11.9\text{ kWh/kg}_{H_2}$ , corresponding to case B19),  $\eta_{\text{round-trip}}$  would go down to  $22.7\%$  and the energy consumption of the  $LH_2$  facility would take  $20\%$  of the total energy demand of the power-to-power storage system.

It becomes clear that the second most influential driver energy-wise is storage and, in this regard, hydrogen liquefaction brings about a substantial  $\eta_{\text{round-trip}}$  reduction. Thus, for on-site or nearby consumption within a short distance,  $LH_2$  is not of interest given that the increase in  $H_2$  density does not offset the much higher energy consumption of the hydrogen-conditioning process. In addition, even though economic aspects are not considered in this study, the implementation of a hydrogen liquefaction plant would expectedly have a negative impact on the total capital cost of the storage facility.

As far as the other electrolyser technologies are concerned (AEC or PEMEC), their round-trip efficiencies are fairly similar due to their comparable specific energy consumption,  $52.3$  and  $53.4\text{ kWh/kg}_{H_2}$  (Fig. 7), and they experience the same fluctuations when different storage media are considered (Fig. 9): efficiency lower than  $20\%$  for  $LH_2$  and around  $21$ – $22\%$  for compressed- $H_2$  or MH. Furthermore, the specific energy consumption of these electrolysers also changes when the operating conditions of the electrolyser change, regardless of the technology of choice (Eq. (3)), and when different materials or integration layouts are adopted. This latter aspect was reported in Table 3 before.

### Economics of power-to-power EES

Engineering project appraisal requires profound understanding of capital (CapEx) and operating (OpEx) expenditures. Regarding CapEx of a P2P system, detailed information about several systems is mandatory, from renewable energy technologies like wind power or solar photovoltaics to electrolysers, hydrogen storage and transportation/distribution, and also power generation systems. Such data are nevertheless scarce given the early stage of development of most hydrogen technologies [94], most of them not fully commercialised yet, and when available they incorporate a large deal of uncertainty. The same applies to OpEx, for which electricity is the primary driver, depending largely on the particular characteristics of each country.

Accordingly, the economics of P2P systems require a dedicated assessment, once the technical features of these systems are more advanced. This is why such assessment is left out of this work, where the focus has been put on the thermodynamic analysis of an early energy storage concept with the aim to assess its competitiveness against other forms of energy storage. Further work by the authors and other researchers in the context of the NextMGT [95] project will focus on this.

### Discussion of results

Power-to-Hydrogen-to-Power energy storage is one of the most promising energy storage options for long-term storage (weeks to months), where pumped hydro storage is the only mature option today, accounting for  $96\%$  of the total energy storage capacity. Moreover, hydrogen, an energy carrier, can be used not only as a means to store renewable energy but also as fuel for mobility and heat generation, and as feed-stock for industries such as ammonia production. This wide portfolio of potential applications of hydrogen has the potential to contribute largely to build a powerful and decarbonised energy economy in the future.

The paper has discussed that, for power-to-power energy storage solutions, three types of electrolysers can be used to

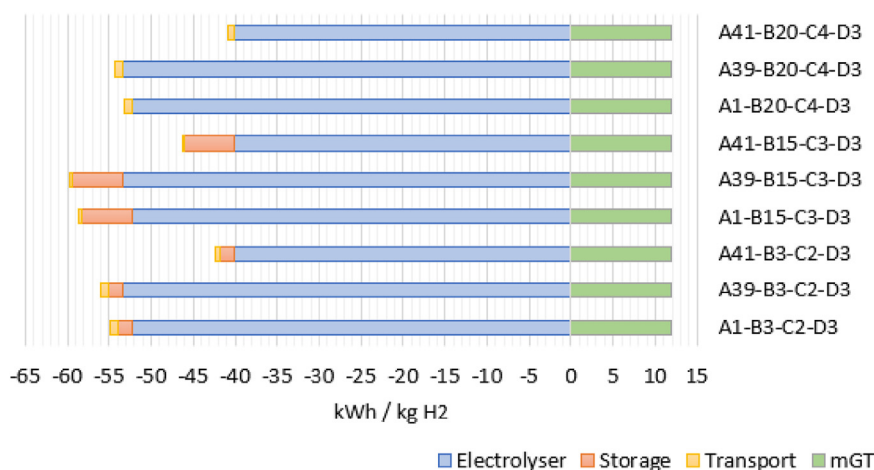
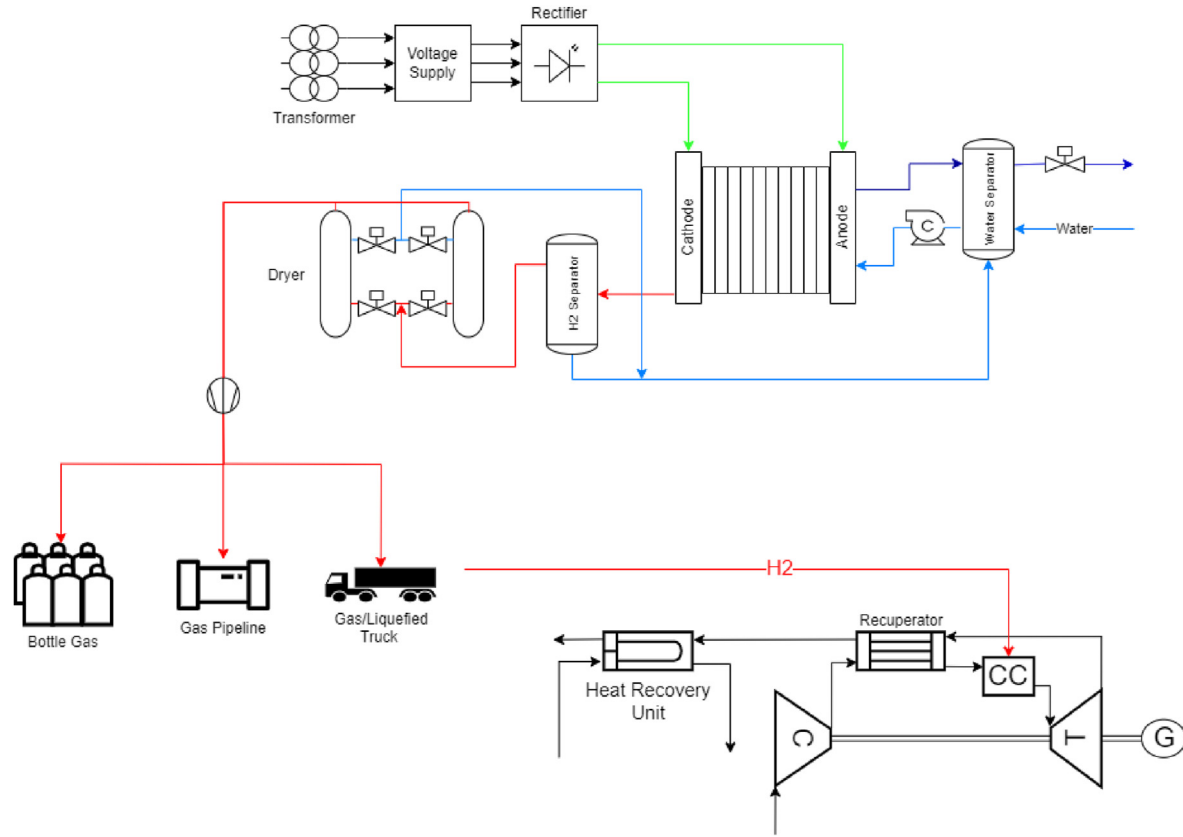


Fig. 7 – Energy balance for the P2P solutions considered.



**Fig. 8 – Considered layout of the Power-to-Power energy storage system based on mGT technology. Colour code: red-hydrogen, blue-water, green-power; dark blue-oxygen. (For interpretation of the references to colour in this figure legend, the reader is referred to the Web version of this article.)**

convert surplus renewable electricity into hydrogen and they all are experiencing substantial technical progress leading to better performances, larger scales and lower costs: AEC, PEMEC and SOEC.

Hydrogen storage can be enabled in three different states: compressed-H<sub>2</sub>, liquefied-H<sub>2</sub> and in the form of metal hydride. Compressed-H<sub>2</sub> requires high-pressure storage vessels (type III & IV [96]) and a compression system able to handle high pressure ratios (> 10:1), what translates into high capital and operating costs. Nevertheless, if the hydrogen production and consumption nodes are at the same location and sufficient

space (land area) is available, lower storage pressures can be used, making this option very attractive. Liquefied-H<sub>2</sub> features a much higher density ( $\approx 78 \text{ kg/m}^3$ ) but the process to liquefy hydrogen is highly energy intensive, making this option attractive only when long-distance transportation is required, for instance between continents. Metal hydrides enable the highest density among the different H<sub>2</sub> storage systems (> 115 kgH<sub>2</sub>/m<sup>3</sup>) but the associated hydrogen release rates are lower than for the other technologies. If this is not a limiting factor and low system weight is not required, then metal hydrides yield the benefit of being a lower energy intensive

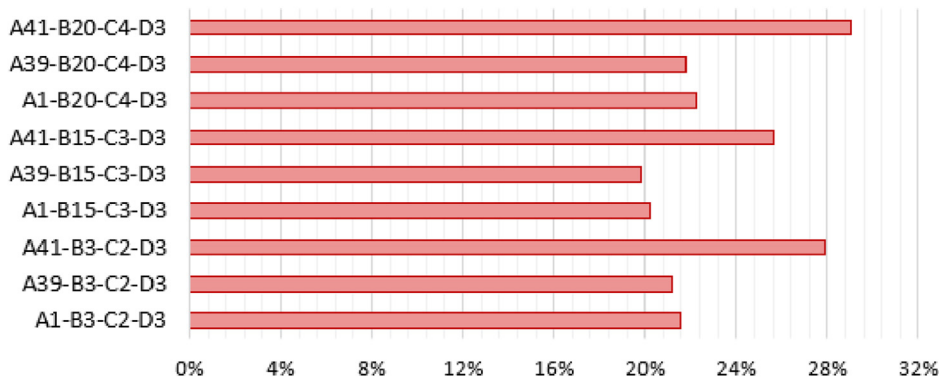


**Fig. 9 – Round-trip efficiency for the P2P solutions presented in Fig. 8.**



process to store H<sub>2</sub>. Yet, given that there exist many types of metal hydrides, it is very important to select the right MH type for each particular application, due to its dependence on heat supply.

Regardless of the storage technology, higher H<sub>2</sub> densities lead to lower energy cost of hydrogen transportation/distribution. Therefore, the volume available for transportation of H<sub>2</sub> sets a strong constraint, either in the form of high-pressure tubes, liquefied-H<sub>2</sub> tanks or truck size limitations. If a FCET is considered, around 3840 kg of LH<sub>2</sub> can be transported in a single trip, which is around four times the energy that can be transported when considering compressed-H<sub>2</sub> or MH.

Stored energy is eventually discharged in the form of electric power when requested by the grid or end-user. For the concept considered in this work, this is done through hydrogen combustion in a micro gas turbine, which stems as a compact, efficient, economical and very fast-responding power generation technology. Indeed, micro gas turbine are able to run at full capacity just a few minutes after start-up and their electric efficiency ranges from 25% for the smaller units (<100 kWe) to almost 40% for engines in the larger output range (≈500 kWe). This efficiency is lower than other power generation technologies such as fuel cells (>55%) or reciprocating internal combustion engines (>45%), but mGTs offer additional, beneficial features such as available high grade heat for Combined Heat and Power (>250°C).

The paper has discussed the critical figure of merit used to determine the viability of an energy storage system, round-trip efficiency ( $\eta_{\text{round-trip}}$ ), which determines the amount of energy that is given back to the grid in comparison with the energy taken originally. Calculations for various configurations of the selected system have shown that the maximum  $\eta_{\text{round-trip}}$  achievable is below 30% and this applies to a system based on the smart integration of a Solid Oxide Electrolyser (SOEC) for H<sub>2</sub> production, compressed-H<sub>2</sub> storage and micro gas turbine (mGT). If AEC or PEMEC were used in lieu of an SOEC,  $\eta_{\text{round-trip}}$  would go down to around 22% at best. This  $\eta_{\text{round-trip}}$  is lower than for other energy storage technologies [97–99]:

1. Pumped-hydro: from 65% in older installations to 75–85% in modern facilities.
2. Flywheels: 80%–90%.
3. Batteries: 75%–85%.
4. Electro-thermal: 65%–75%.
5. Compressed air: 45%–70%.
6. Liquid Air: 30%–70%.<sup>4</sup>

The aforesaid energy storage technologies have considerably higher  $\eta_{\text{round-trip}}$  than power-to-power systems based on micro gas turbines (mGT-P2P). However, only hydro, compressed-air storage (CAES) and liquid air storage (LAES) are comparable to mGT-P2P (or, in general, GT-P2P) in their capacity to store energy for days or even months at a larger scale. Additionally, the critical advantage of the mGT-P2P option over these technologies is that it is independent from geographical constraints and it can be installed almost anywhere where renewable electricity and water are available in

addition to the advantage of dealing with an energy vector as it is hydrogen. Hence, despite having  $\eta_{\text{round-trip}} \approx 29\%$ , it is the only *fully flexible* (installation wise) large-scale, long-term energy storage solution that can be installed virtually anywhere where there is a need for energy storage. Additionally, it also provides a high-grade heat source which makes it suitable for CHP applications.

Finally, it is to note that in spite of the maximum  $\eta_{\text{round-trip}}$  of around 30% reported in this work for mGT-P2P energy storage solutions, there is still a large margin for improvement. This potential is found in the hydrogen production and power generation stages of the system. In particular, the operation of an ideal electrolyser with null losses would require 33.33 kWh/kg<sub>H<sub>2</sub></sub>, what translates into a potential 13–15% gain in  $\eta_{\text{round-trip}}$ . Even if this is a theoretical limit that cannot be achieved in practice, predictions from different world energy organisations [17,37,38] estimate that the energy consumption of electrolysers is expected to decrease by a few kWh/kg<sub>H<sub>2</sub></sub> in the next decade, leading to a  $\Delta\eta_{\text{round-trip}}$  improvement of around 3–5% (one third of the theoretical efficiency gain). Parallel to this, an even larger performance enhancement could come from further improvements in micro gas turbine technology. Indeed, the efficiency of these engines could increase to around 40% [92,100] in the next decade and the combination of SOEC/SOFC and mGT in so-called hybrid systems would boost power generation efficiencies to values as high as 55–60% [101]. The cumulative effect of this foreseen progress on the performance of mGT-P2P technology would translate into  $\eta_{\text{round-trip}}$  higher than 40–42% in the next decade. This would take this technology closer to and beyond cost-effectiveness, setting it on the map of essential technologies to enable carbon neutrality by 2050.

## Conclusions

The paper considers that, for power-to-power energy storage solutions, three types of electrolysers can be used to convert surplus renewable electricity into hydrogen: AEC, PEMEC and SOEC. This hydrogen can then be stored in three different states: compressed-H<sub>2</sub>, liquefied-H<sub>2</sub> and in the form of metal hydride; regardless of the storage technology, higher H<sub>2</sub> densities lead to lower energy costs of hydrogen transportation/distribution. Finally, stored energy is eventually discharged in the form of electric power when requested by the grid or end-user. For the concept considered in this work, this is done through hydrogen combustion in a micro gas turbine (≤500 kWe).

The paper has discussed round-trip efficiency ( $\eta_{\text{round-trip}}$ ) as the critical figure of merit to determine the viability of an energy storage system. The aim of the study is to offer a comprehensive analysis of the options available for each of the systems implied in a P2P-mGT, using round-trip efficiency as the figure of merit for comparison. This leads to certain limitations, mostly coming from the numerous power and heat streams of each subsystem that must be integrated into the optimisation process, which cannot be covered in detail in this work due to length limitations. Therefore, this study is a first step towards achieving highly efficient and optimised layouts for P2P-mGT energy storage systems, whose results

<sup>4</sup> if it considers hot/cold recycle [99].

will narrow the design space for future, refined analysis of components. Calculations for various configurations of the selected system have shown that the maximum  $\eta_{\text{round-trip}}$  achievable is below 30%, for the time being, and this applies to a system based on the smart integration of a Solid Oxide Electrolyser (SOEC) for H<sub>2</sub> production, compressed-H<sub>2</sub> storage and micro gas turbine (mGT). If AEC or PEMEC were used in lieu of an SOEC,  $\eta_{\text{round-trip}}$  would go down to around 22% at best.

Finally, it is to note that in spite of the maximum  $\eta_{\text{round-trip}}$  of around 30% reported in this work for mGT-P2P energy storage solutions, there is still a large margin for improvement. The largest potential is found in the hydrogen production and power generation stages of the system. Improvements in these systems could lead to  $\eta_{\text{round-trip}}$  of around 40–42% in the next decade.

### Declaration of competing interest

The authors declare that they have no known competing financial interests or personal relationships that could have appeared to influence the work reported in this paper.

### Acknowledgment

This work has been developed in the frame of the Next Generation of Micro Gas Turbines for High Efficiency, Low Emissions and Fuel Flexibility, NextMGT, which has received funding from the European Union's Horizon 2020 research and innovation programme under Marie Skłodowska-Curie grant agreement No 861079.

The University of Seville is also gratefully acknowledged for supporting this research through its Internal Research Programme (Plan Propio de Investigación), under contract No 2019/00000359.

### REFERENCES

- [1] IEA. Renewables 2020. URL, <https://www.iea.org/reports/renewables-2020>; 2020.
- [2] IRENA. Global renewables outlook: energy transformation 2050 (2020). URL, <https://www.irena.org/publications/2020/Apr/Global-Renewables-Outlook-2020>.
- [3] IRENA, Innovation landscape brief. Advanced forecasting of variable renewable power generation. URL, [https://www.irena.org/-/media/Files/IRENA/Agency/Publication/2020/Jul/IRENA\\_Advanced\\_weather\\_forecasting\\_2020.pdf?la=en&hash=8384431B56569C0D8786C9A4FDD56864443D10AF](https://www.irena.org/-/media/Files/IRENA/Agency/Publication/2020/Jul/IRENA_Advanced_weather_forecasting_2020.pdf?la=en&hash=8384431B56569C0D8786C9A4FDD56864443D10AF); 2020.
- [4] Mathiesen B, Lund H, Connolly D, Wenzel H, Østergaard P, Möller B, Nielsen S, Ridjan I, Karnøe P, Sperling K, Hvelplund F. Smart energy systems for coherent 100 % renewable energy and transport solutions. *Appl Energy* 2015;145:139–54. <https://doi.org/10.1016/j.apenergy.2015.01.075>.
- [5] Koirala B, Hers S, Morales-España G, Özdemir Özge, Sijm J, Weeda M. Integrated electricity, hydrogen and methane system modelling framework: application to the Dutch infrastructure outlook 2050. *Appl Energy* 2021;289:116713. <https://doi.org/10.1016/j.apenergy.2021.116713>.
- [6] Michael Sterner IS. *Handbook of energy storage*. Springer-Verlag Berlin Heidelberg; 2019.
- [7] Aneke M, Wang M. Energy storage technologies and real life applications – a state of the art review. *Appl Energy* 2016;179:350–77. <https://doi.org/10.1016/j.apenergy.2016.06.097>.
- [8] IRENA. Electricity storage and renewables. URL, <https://www.irena.org/publications/2017/Oct/Electricity-storage-and-renewables-costs-and-markets>; 2017.
- [9] Budt M, Wolf D, Span R, Yan J. A review on compressed air energy storage: basic principles, past milestones and recent developments. *Appl Energy* 2016;170:250–68. <https://doi.org/10.1016/j.apenergy.2016.02.108>.
- [10] Council H. Path to hydrogen competitiveness: a cost perspective. 2020. URL, <https://hydrogencouncil.com/en/path-to-hydrogen-competitiveness-a-cost-perspective/>.
- [11] Thema M, Bauer F, Sterner M. Power-to-gas: electrolysis and methanation status review. *Renew Sustain Energy Rev* 2019;112:775–87. <https://doi.org/10.1016/j.rser.2019.06.030>.
- [12] Wulf C, Linßen J, Zapp P. Review of power-to-gas projects in europe. *Energy Proc* 2018;155:367–78. <https://doi.org/10.1016/j.egypro.2018.11.041>. 12th International Renewable Energy Storage Conference, IRES 2018, 13-15 March 2018, Düsseldorf, Germany.
- [13] Cells F, Undertaking HJ. Hydrogen roadmap europe: a sustainable pathway for the european energy transition. URL, <https://www.fch.europa.eu/publications/hydrogen-roadmap-europe-sustainable-pathway-european-energy-transition>; Jan. 2019.
- [14] FCHEA. Road map to a us hydrogen economy. Dec. 2020.
- [15] Hydrogen, F. C. S. Council. The strategic road map for hydrogen and fuel cells. Mar. 2019.
- [16] G. o. C. Ministry of Energy. National green hydrogen strategy. URL, [https://energia.gov.cl/sites/default/files/national\\_green\\_hydrogen\\_strategy\\_-\\_chile.pdf](https://energia.gov.cl/sites/default/files/national_green_hydrogen_strategy_-_chile.pdf); Nov. 2020.
- [17] I. E. A. (IEA). The future of hydrogen. URL, <https://www.iea.org/reports/the-future-of-hydrogen>; 2019.
- [18] ACES. Advanced clean energy storage. URL, [https://power.mhi.com/regions/amer/news/190530.html?utm\\_source=amerweb&utm\\_medium=release&utm\\_campaign=DOE](https://power.mhi.com/regions/amer/news/190530.html?utm_source=amerweb&utm_medium=release&utm_campaign=DOE). [Accessed 25 October 2021].
- [19] ROBINSON-H2020. Smart integration of local energy sources and innovative storage for flexible, secure and cost-efficient energy supply on industrialized islands. URL, <https://www.robinson-h2020.eu/>. [Accessed 25 March 2021].
- [20] Green Hysland project planned for mallorca. *Fuel Cell Bull* 2020;11:9–10. [https://doi.org/10.1016/S1464-2859\(20\)30521-6](https://doi.org/10.1016/S1464-2859(20)30521-6). 2020.
- [21] FLEXnCONFU-H2020. Flexibilize combined cycle power plant through power-to-x solutions using non-conventional fuels. URL, <https://flexnconfu.eu/>. [Accessed 25 March 2021].
- [22] HYFLEXPOWER-H2020. Hydrogen as a flexible energy storage for a fully renewable european power system. URL, <https://cordis.europa.eu/project/id/884229>. [Accessed 25 March 2021].
- [23] Heymann F, Rüdüsüli M, vom Scheidt F, Camanho AS. Performance benchmarking of power-to-gas plants using composite indicators. *Int J Hydrogen Energy* 2021. <https://doi.org/10.1016/j.ijhydene.2021.10.189>.
- [24] Crespi E, Colbertaldo P, Guandalini G, Campanari S. Design of hybrid power-to-power systems for continuous clean pv-based energy supply. *Int J Hydrogen Energy* 2021;46(26):13691–708. <https://doi.org/10.1016/j.ijhydene.2020.09.152>. european Fuel Cell Conference & Exhibition 2019.

- [25] Loisel R, Baranger L, Chemouri N, Spinu S, Pardo S. Economic evaluation of hybrid off-shore wind power and hydrogen storage system. *Int J Hydrogen Energy* 2015;40(21):6727–39. <https://doi.org/10.1016/j.ijhydene.2015.03.117>.
- [26] T. Bexten, T. Sieker, M. Wirsum, Techno-economic analysis of a hydrogen production and storage system for the on-site fuel supply of hydrogen-fired gas turbines, *J Eng Gas Turbines Power* 143 (12). doi:10.1115/1.4052023.
- [27] Mukelabai MD, Gillard JM, Patchigolla K. A novel integration of a green power-to-ammonia to power system: reversible solid oxide fuel cell for hydrogen and power production coupled with an ammonia synthesis unit. *Int J Hydrogen Energy* 2021;46(35):18546–56. <https://doi.org/10.1016/j.ijhydene.2021.02.218>.
- [28] Wang L, Zhang Y, Pérez-Fortes M, Aubin P, Lin T-E, Yang Y, Maréchal F, Van herle J. Reversible solid-oxide cell stack based power-to-x-to-power systems: comparison of thermodynamic performance. *Appl Energy* 2020;275:115330. <https://doi.org/10.1016/j.apenergy.2020.115330>.
- [29] Ishaq H, Dincer I, Naterer GF. Performance investigation of an integrated wind energy system for co-generation of power and hydrogen. *Int J Hydrogen Energy* 2018;43(19):9153–64. <https://doi.org/10.1016/j.ijhydene.2018.03.139>.
- [30] Motahar S, Alemrajabi AA. Exergy based performance analysis of a solid oxide fuel cell and steam injected gas turbine hybrid power system. *Int J Hydrogen Energy* 2009;34(5):2396–407. <https://doi.org/10.1016/j.ijhydene.2008.12.065>.
- [31] Alirahmi SM, Assareh E, Chitsaz A, Ghazanfari Holagh S, Jalilinasrabad S. Electrolyzer-fuel cell combination for grid peak load management in a geothermal power plant: power to hydrogen and hydrogen to power conversion. *Int J Hydrogen Energy* 2021;46(50):25650–65. <https://doi.org/10.1016/j.ijhydene.2021.05.082>.
- [32] Tukenmez N, Yilmaz F, Ozturk M. A thermal performance evaluation of a new integrated gas turbine-based multigeneration plant with hydrogen and ammonia production. *Int J Hydrogen Energy* 2021;46(57):29012–26. <https://doi.org/10.1016/j.ijhydene.2020.11.054>. HYDROGEN ENERGY SYSTEMS.
- [33] E. Comission. Paris agreement. URL, [https://ec.europa.eu/clima/policies/international/negotiations/paris\\_en#tab=0-0](https://ec.europa.eu/clima/policies/international/negotiations/paris_en#tab=0-0). [Accessed 18 March 2021].
- [34] Gabrielli P, Charbonnier F, Guidolin A, Mazzotti M. Enabling low-carbon hydrogen supply chains through use of biomass and carbon capture and storage: a swiss case study. *Appl Energy* 2020;275:115245. <https://doi.org/10.1016/j.apenergy.2020.115245>.
- [35] Nikolaidis P, Poullikkas A. A comparative overview of hydrogen production processes. *Renew Sustain Energy Rev* 2017;67:597–611. <https://doi.org/10.1016/j.rser.2016.09.044>.
- [36] Dawood F, Anda M, Shafiqullah G. Hydrogen production for energy: an overview. *Int J Hydrogen Energy* 2020;45(7):3847–69. <https://doi.org/10.1016/j.ijhydene.2019.12.059>.
- [37] IRENA. Green hydrogen cost reduction. URL, <https://irena.org/publications/2020/Dec/Green-hydrogen-cost-reduction;2020>.
- [38] Morante JR, Andreu T, García G, Guilera J, Tarancón A, Torrell M. Hidrógeno: vector energético de una economía descarbonizada. Fundación Naturgy 2020. URL, <https://www.fundacionnaturgy.org/publicacion/hidrogeno-vector-energetico-de-una-economia-descarbonizada/>.
- [39] Godula-Jopek A. Hydrogen production. John Wiley & Sons, Ltd; 2015. <https://doi.org/10.1002/9783527676507.ch1>.
- [40] Schmidt O, Gambhir A, Staffell I, Hawkes A, Nelson J, Few S. Future cost and performance of water electrolysis: an expert elicitation study. *Int J Hydrogen Energy* 2017;42(52):30470–92. <https://doi.org/10.1016/j.ijhydene.2017.10.045>.
- [41] Flexible combined production of power, heat and transport fuels from renewable energy sources. URL, <https://ec.europa.eu/research/participants/documents/downloadPublic?documentIds=080166e5bd5eb58c&appId=PPGMS;2018>.
- [42] Millet P. Fundamentals of water electrolysis. John Wiley & Sons, Ltd; 2015. p. 33–62. <https://doi.org/10.1002/9783527676507.ch2>. Ch. 2.
- [43] Eichman J, Harrison K, Peters M. Novel electrolyzer applications: providing more than just hydrogen. National Renewable Energy Lab. (NREL) 2014. <https://doi.org/10.2172/1159377.NREL/TP-5400-61758>.
- [44] Sunfire. Sunfire hydrogen electrolyzer. URL, <https://www.sunfire.de/en/hydrogen>. [Accessed 19 March 2021].
- [45] Enapter. Enapter hydrogen electrolyzer. URL, <https://www.enapter.com/electrolyser>. [Accessed 19 March 2021].
- [46] Green Hydrogen. Green hydrogen hydrogen electrolyzer. URL, <https://greenhydrogen.dk/#electrolyzers>. [Accessed 19 March 2021].
- [47] McPhy. McPhy hydrogen electrolyzer. URL, <https://mcphy.com/en/equipment-services/electrolyzers/>. [Accessed 19 March 2021].
- [48] Nel Hydrogen. Nel hydrogen hydrogen electrolyzer. URL, [https://nelhydrogen.com/water-electrolysers-hydrogen-generators/?gclid=Cj0KCQjw19GCBhDvARIsAFunhsnLZjZNkEVldj2L1FS6\\_UFlviwP3GVpA9S9m3t5rSa5GMjwYfptfroaAsrjEALw\\_wcB](https://nelhydrogen.com/water-electrolysers-hydrogen-generators/?gclid=Cj0KCQjw19GCBhDvARIsAFunhsnLZjZNkEVldj2L1FS6_UFlviwP3GVpA9S9m3t5rSa5GMjwYfptfroaAsrjEALw_wcB). [Accessed 19 March 2021].
- [49] ITM Power. ITM power hydrogen electrolyzer. URL, <https://www.itm-power.com/products>. [Accessed 19 March 2021].
- [50] Neuman & Esser Group. Hydrogen compressors. URL, <https://www.neuman-esser.de/en/compressors/hydrogen-compressors/>. [Accessed 19 March 2021].
- [51] Mokhatab S, Poe WA. Chapter 11 - natural gas compression. In: Mokhatab S, Poe WA, editors. Handbook of natural gas transmission and processing (second edition). 2nd ed. Edition. Boston: Gulf Professional Publishing; 2012. p. 393–423. <https://doi.org/10.1016/B978-0-12-386914-2.00011-X>.
- [52] N. I. of Standards, T. (NIST). Hydrogen compressibility at different temperatures and pressures. URL, <https://h2tools.org/hyarc/hydrogen-data/hydrogen-compressibility-different-temperatures-and-pressures>. [Accessed 25 October 2021].
- [53] Sdanghi G, Maranzana G, Celzard A, Fierro V. Review of the current technologies and performances of hydrogen compression for stationary and automotive applications. *Renew Sustain Energy Rev* 2019;102:150–70. <https://doi.org/10.1016/j.rser.2018.11.028>.
- [54] Bell IH, Wronski J, Quoilin S, Lemort V. Pure and pseudo-pure fluid thermophysical property evaluation and the open-source thermophysical property library coolprop. *Ind Eng Chem Res* 2014;53(6):2498–508. <https://doi.org/10.1021/ie4033999>.
- [55] Walnum H, Berstad D, Drescher M, Nekså P, Quack H, Haberstroh C, Essler J. Principles for the liquefaction of hydrogen with emphasis on precooling processes. *Refrigeration Science and Technology* 2012;2012:273–80.
- [56] Petitpas G. Simulation of boil-off losses during transfer at a lh2 based hydrogen refueling station. *Int J Hydrogen Energy* 2018;43(46):21451–63. <https://doi.org/10.1016/j.ijhydene.2018.09.132>.
- [57] IDEALHY. Idealhy (grant agreement no. 278177). URL, <https://www.idealhy.eu/>. [Accessed 22 March 2021].

- [58] Decker L, Bracha M. *Grosstechnische wasserstoffverflüssigung in leuna, tagung*; 35, deutscher kalte- und klimatechnischer verein; dkv-tagungsbericht 2008. In: Deutscher Kalte- und Klimatechnischer Verein; DKV-Tagungsbericht 2008, DKV TAGUNGSBERICHT, Tagung; 35, Deutscher Kalte- und Klimatechnischer Verein; DKV-Tagungsbericht 2008, vol. 35. Hannover: DKV; 2008. p. 455–60.
- [59] Cardella U, Decker L, Klein H. Roadmap to economically viable hydrogen liquefaction. *Int J Hydrogen Energy* 2017;42(19):13329–38. <https://doi.org/10.1016/j.ijhydene.2017.01.068>. special Issue on The 21st World Hydrogen Energy Conference (WHEC 2016), 13-16 June 2016, Zaragoza, Spain.
- [60] Cardella U, Decker L, Klein H. Economically viable large-scale hydrogen liquefaction. In: IOP conference series: materials science and engineering, vol. 171; 2017. p. 12013. <https://doi.org/10.1088/1757-899x/171/1/012013>.
- [61] Baker C, Shaner R. A study of the efficiency of hydrogen liquefaction. *Int J Hydrogen Energy* 1978;3(3):321–34. [https://doi.org/10.1016/0360-3199\(78\)90037-X](https://doi.org/10.1016/0360-3199(78)90037-X).
- [62] Fukano T, Yamashita N, Ohira K. A study of the large hydrogen liquefaction process. *J High Pres Inst Jpn* 2000;38(5):298–305. <https://doi.org/10.11181/hpi1972.38.298>.
- [63] Quack Hans. Conceptual design of a high efficiency large capacity hydrogen liquefier. *AIP Conf. Proc.* 2002;613. <https://doi.org/10.1063/1.1472029>.
- [64] K O. A summary of liquid hydrogen and cryogenic technologies in Japan's we-net project. In: AIP conference proceedings, vol. 710; 2004. p. 27–34. <https://doi.org/10.1063/1.1774663>.
- [65] M. A. Shimko, Iii.7 innovative hydrogen liquefaction cycle, FY 2008 Annual Progress Report, DOE Hydrogen Program.
- [66] Macchi E, Valenti G. *Liquid hydrogen: from clean coal to filling station. part a: proposal on an innovative, highly-efficient, large-scale liquifier.* 2007.
- [67] Berstad DO, Stang JH, Nekså P. Large-scale hydrogen liquefier utilising mixed-refrigerant pre-cooling. *Int J Hydrogen Energy* 2010;35(10):4512–23. <https://doi.org/10.1016/j.ijhydene.2010.02.001>. novel Hydrogen Production Technologies and Applications.
- [68] R G, W O, A P, M W. *Liquid hydrogen for europe - the linde plant at ingolstadt. fluessigwasserstoff fuer europa - die linde-anlage in ingolstadt.* Jan 1994.
- [69] Voth R, Parrish W. *Studies of hydrogen liquefier efficiency and the recovery of the liquefaction energy.* Cryogenics Division, Institute for Basic Standards, National Bureau of Standards; 1977.
- [70] Calabrese M, Douglas K, Orinstein B, Vasansiri K, Wang M. *Heat recovery from natural gas liquefaction process.* 04 2012.
- [71] Yu X, Tang Z, Sun D, Ouyang L, Zhu M. Recent advances and remaining challenges of nanostructured materials for hydrogen storage applications. *Prog Mater Sci* 2017;88:1–48. <https://doi.org/10.1016/j.pmatsci.2017.03.001>.
- [72] Chung C, Yang S-W, Yang C-Y, Hsu C-W, Chiu P-Y. Experimental study on the hydrogen charge and discharge rates of metal hydride tanks using heat pipes to enhance heat transfer. *Appl Energy* 2013;103:581–7. <https://doi.org/10.1016/j.apenergy.2012.10.024>.
- [73] Godula-Jopek A, Jehle W, Wellnitz J. *Hydrogen storage technologies.* John Wiley & Sons; 2012. Incorporated.
- [74] Ye Y, Ding J, Wang W, Yan J. The storage performance of metal hydride hydrogen storage tanks with reaction heat recovery by phase change materials. *Appl Energy* 2021;299:117255. <https://doi.org/10.1016/j.apenergy.2021.117255>.
- [75] Han G, Kwon Y, Kim JB, Lee S, Bae J, Cho E, Lee BJ, Cho S, Park J. Development of a high-energy-density portable/mobile hydrogen energy storage system incorporating an electrolyzer, a metal hydride and a fuel cell. *Appl Energy* 2020;259:114175. <https://doi.org/10.1016/j.apenergy.2019.114175>.
- [76] HBank. Metal hydride for hydrogen storage products. URL, <http://www.hbank.com.tw/fuelcell.html>.
- [77] P. Industries. Metal hydride for hydrogen storage products. URL, <https://www.pragma-industries.com/hydrogen-storage/>.
- [78] h2planet. Metal hydride for hydrogen storage products. URL, <https://www.h2planet.eu/en/products/professional/Hydrogenstorage>.
- [79] Hyundai. Xcient fuel cell truck. URL, <https://trucknbus.hyundai.com/global/en/products/truck/xcient-fuel-cell>. [Accessed 31 March 2021].
- [80] hydrexia. Ground storage products. URL, <http://hydrexia.com/hydrexia-hydrogen-storage-technology>. [Accessed 23 March 2021].
- [81] Calvera. High-pressure hydrogen mobility unit products. URL, <https://www.calvera.es/productos/>. [Accessed 5 April 2021].
- [82] Lucia U. Overview on fuel cells. *Renew Sustain Energy Rev* 2014;30:164–9. <https://doi.org/10.1016/j.rser.2013.09.025>.
- [83] Taamallah S, Vogiatzaki K, Alzahrani F, Mokheimer E, Habib M, Ghoniem A. Fuel flexibility, stability and emissions in premixed hydrogen-rich gas turbine combustion: technology, fundamentals, and numerical simulations. *Appl Energy* 2015;154:1020–47. <https://doi.org/10.1016/j.apenergy.2015.04.044>.
- [84] Meziane S, Bentebbiche A. Numerical study of blended fuel natural gas-hydrogen combustion in rich/quench/lean combustor of a micro gas turbine. *Int J Hydrogen Energy* 2019;44(29):15610–21. <https://doi.org/10.1016/j.ijhydene.2019.04.128>.
- [85] Shih H-Y, Liu C-R. A computational study on the combustion of hydrogen/methane blended fuels for a micro gas turbines. *Int J Hydrogen Energy* 2014;39(27):15103–15. <https://doi.org/10.1016/j.ijhydene.2014.07.046>.
- [86] di Gaeta A, Reale F, Chiariello F, Massoli P. A dynamic model of a 100 kw micro gas turbine fuelled with natural gas and hydrogen blends and its application in a hybrid energy grid. *Energy* 2017;129:299–320. <https://doi.org/10.1016/j.energy.2017.03.173>.
- [87] E. T. N. (ETN). Hydrogen gas turbines. URL, <https://etn.global/wp-content/uploads/2020/02/ETN-Hydrogen-Gas-Turbines-report.pdf>; 2020.
- [88] Magazine GTW. Decarbonizing gas turbines via hydrogen fuel. URL, <https://gasturbineworld.com/decarbonizing-gas-turbines-via-hydrogen-fuel/>. [Accessed 24 March 2021].
- [89] Corporation CT. Capstone products. URL, <https://www.capstoneturbine.com/products>. [Accessed 24 March 2021].
- [90] Solutions FE. Flex energy turbines. URL, <https://www.flexenergy.com/turbine-innovations/>. [Accessed 24 March 2021].
- [91] Energia A. Ansaldo energia microturbine ae-100. URL, <https://www.ansaldoenergia.com/business-lines/new-units/microturbines>. [Accessed 24 March 2021].
- [92] Turbines A. Aurelia microturbine a400. URL, <https://aureliaturbines.com/company/business>. [Accessed 24 March 2021].
- [93] M. T. T. B.V.. Mtt enertwin. URL, <https://enertwin.com/enertwin/>. [Accessed 24 March 2021].
- [94] IEA. Energy technology perspectives 2020. <https://doi.org/10.1787/ab43a9a5-en>; 2020.

- [95] NEXTMGT. H2020 nextmgt (grant agreement no. 861079). URL, <https://www.nextmgt.com/>.
- [96] Barthelemy H, Weber M, Barbier F. Hydrogen storage: recent improvements and industrial perspectives. *Int J Hydrogen Energy* 2017;42(11):7254–62. <https://doi.org/10.1016/j.ijhydene.2016.03.178>.
- [97] IRENA. Renewable power-to-hydrogen. URL, [https://www.irena.org/-/media/Files/IRENA/Agency/Publication/2019/Sep/IRENA\\_Power-to-Hydrogen\\_Innovation\\_2019.pdf](https://www.irena.org/-/media/Files/IRENA/Agency/Publication/2019/Sep/IRENA_Power-to-Hydrogen_Innovation_2019.pdf); 2019.
- [98] E. blog (ESS). Round-trip efficiency for ess. URL, <https://energymag.net/round-trip-efficiency/>. [Accessed 25 March 2021].
- [99] Vecchi A, Li Y, Ding Y, Mancarella P, Sciacovelli A. Liquid air energy storage (laes): a review on technology state-of-the-art, integration pathways and future perspectives. *Advances in Applied Energy* 2021;3:100047. <https://doi.org/10.1016/j.adapen.2021.100047>.
- [100] De Paepe W, Montero Carrero M, Bram S, Parente A, Contino F. Towards higher micro gas turbine efficiency and flexibility — humidified mgts: a review. *J Eng Gas Turbines Power* 2018;140(8). <https://doi.org/10.1115/1.4038365>.
- [101] Damo U, Ferrari M, Turan A, Massardo A. Solid oxide fuel cell hybrid system: a detailed review of an environmentally clean and efficient source of energy. *Energy* 2019;168:235–46. <https://doi.org/10.1016/j.energy.2018.11.091>.